EXPERIMENTAL AND NUMERICAL INVESTIGATIONS OF PULL-OUT STRENGTH OF TIMBER JOINTS WITH GLUED-IN RODS

by

PEDRAM FAGHANI

B.Sc., (Civil Engineering), The University of Tehran, 2010

A THESIS SUBMITTED IN PARTIAL FULFILLMENT OF THE REQUIREMENTS FOR THE DEGREE OF

MASTER OF APPLIED SCIENCE

in

The Faculty of Graduate and Postdoctoral Studies
(Civil Engineering)

THE UNIVERSITY OF BRITISH COLUMBIA
(Vancouver)

August, 2013

ABSTRACT

Timber joints with glued-in rods have several advantages with respect to mechanical connections, such as higher stiffness, more uniform stress distribution, less bar corrosion problems and better appearance. This thesis describes experimental and numerical studies of timber joints made with glass fibre reinforced polymer (GFRP) rods glued by polyurethane adhesive (PUR) into glued-laminated timber specimens made of Douglas-fir.

Experimental work was performed at Centre for Advanced Wood Processing of the Wood Science Department and the Materials Laboratory of the Civil Engineering Department at University of British Columbia Vancouver. A total of 125 specimens from 25 different test series with 5 replicates each were tested in tension until failure. The objective of the study was to evaluate the influence of the geometric parameters on the joint performance. The experimental data showed the importance of the rod diameter and anchorage length on the capacity of glued-in rod joints. In all the cases, when increasing the diameter of the bar or anchorage length, the average value of the reached failure load increased; this increase, however, was not linearly proportional to the timber-adhesive interface.

Experimental failure loads have been compared with the theoretical values and in all the cases the experimental results were lower than the theoretical values, which might be because of incompatibilities between the chosen PUR and GRFP rod.

A 3D finite element model was developed using the commercial software package ANSYS 14.0 in order to investigate the stress distribution within the joints. The model was validated and found to be in good agreement with the experimental observations, allowing it to be used for future parameter optimization and the application of numerical capacity prediction methods.

PREFACE

This thesis is original, unpublished, independent work by the author, Pedram Faghani, under supervision of Dr. Thomas Tannert.

TABLE OF CONTENTS

LIST OF TABLES

LIST OF FIGURES

ACKNOWLEDGMENTS

- Dr. Thomas Tannert for his patience, support and valuable comments during the course of this research.
- My dear family and friends for their huge support and encouragement.
- Lawrence Gunther and Vincent Leung for their remarkable help during the experimental period at the Centre for Advanced Wood Processing in the Wood Science Department.
- Mark Rigolo for his significant help at the start of the project and for organizing various meetings.
- John Wong for his remarkable job building the electrical part of experimental system.
- Ken Taggart and Harald Schrempp for building the mechanical parts of the experimental apparatus.
- Amir Garekani for his assistance during experiments.
- NSERC (Natural Sciences and Engineering Research Council of Canada) for financial support of this project.

To my parents

1. INTRODUCTION

1.1 GENERAL INFORMATION

Wood has a long history as a building material. Wood is by far the preferred building material for residential construction in North America. Nowadays, the need to decrease the carbon footprint of civil engineering structures leads to the use of more natural materials such as wood.

In every timber structure, joints are a matter of crucial importance. They constitute a significant portion of the engineering work and remain an area where considerable creativity can be applied. Many different connections are used in timber structures. Different connections are required for different purposes. Connections are influenced by a number of factors including strength, ductility, stiffness, aesthetics, constructability and cost. They must have satisfactory strength and stiffness together with reasonable ductility.

There are many traditional connections techniques in timber engineering, such as bolt and nail connections. However these connections often lack stiffness with respect to bending moments, caused by oversized holes in connections, which does lower the structure's resistance against bending moments. Therefore, new techniques for reliable and moment resisting connections are required. The acceptance of novel timber joints in the structural engineering community, however, depends on the availability of design data, and moreover a procedure to reliably predict its strength.

Glued-in rod timber connections are a promising technique. It is a simple connection system comprised of one or more rods bonded into a timber section using an adhesive. Figure 1.1 illustrates the concept. The first design of timber joints with glued-in rods was applied in Sweden around 1965 [12]. Major work on glued-in steel rods connection was performed by Riberholt in

Denmark [8]. Glued-in rod timber connections were expensive, but good looking and reminiscence of old types of carpenter joints. The technology of connections with glued-in rods started to develop in the 1980s and is still on-going. In practice, however, it is commonly used in few European countries and in Australia and New Zealand [9].

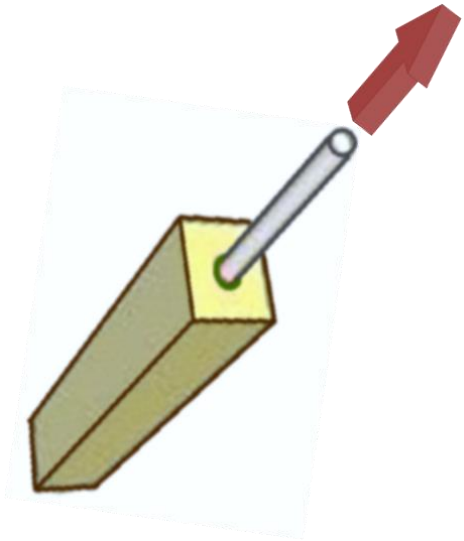

Figure 1.1- Glued-in rod schematic

Glued-in rods, as a subset of adhesive joints, represent a large category of hybrid joints since they involve three materials (timber, rod and adhesive). Different types of rod materials that can be glued into timber are steel rods, fibre reinforced plastic rods, and wooden rods. The most commonly used material for rods is steel, since it permits the design of joints with a ductile failure mode. Another material for rods which is less common is fibre reinforced polymer (FRP). Initial studies on FRP rods were made by Müller and Roth in 1991 [8]. In later investigations, Harvey et al. [13] tested connections with rods made from glass FRP (GFRP) and carbon FRP (CFRP). The results revealed that these materials have some advantages such as ease of manufacturing, light weight and statically efficient connections. However, steel rods have the advantage of yielding; once reaching the yield point, a joint connected with steel rods has still

some load carrying capacity whereas FRP rods behave in a brittle manner. Figure 1.2 shows different types of rods used in glued-in rod connections.

Figure 1.2- Different types of rod; left: Steel, center: GFRP and right: CFRP

Different types of adhesives have been tested in manufacturing of glued-in rod connections. In early years, wood adhesives based on phenol-resorcinol or epoxy (EPX) adhesives were used, but over the years later work has also included the use of polyurethanes (PUR). The most common adhesive types for joints with glued-in rods are 2-component PUR and EPX.

1.2 APPLICATION AND MANUFACTURING

Timber joints with glued-in rods have several applications in structures: either to transfer forces between structural members, or to retrofit damaged parts of timber structures. Glued-in rods act perfectly in several types of moment-resisting timber joints. They can be used in frame nodes and corners of portal frames with a steel bracket to create a moment connection. One main advantage of this joint is that the rods are hidden inside the timber, which is aesthetically beneficial and, moreover, it better protects the connector from possible corrosion and fire. Glued-in rods have two distinct disadvantages. First, they require a high level of quality control during the construction process, and secondly, they have the potential to degrade if the moisture content fluctuates [11]. Typically, the largest unknown in bonded-in rod connections is the adhesive.

The timber joint with glued-in rods is more widely applied in glulam structures, connecting beam and column members. Steel rods are sometimes substituted by timber rods (also called wooden dowels or wooden pegs); the capacity is then reduced [9]. For structural purposes, different types of adhesives have been used to form, for instance, scarf joints, finger joints, lap joints, web joints or connections with glued-in rods. Previous research showed that different types of adhesives could influence the capacity of the timber connections [3].

In timber joints with glued-in rods, rod can be glued into the timber by injecting the adhesive into a provided hole, or by screwing the rod into the timber hole that is prefilled with glue. A sample of test specimens is shown in Figure 1.3. It is essential to pay special attention to the manufacturing of glued-in rods connections, as is the case for all types of adhesive timber joints. The specific usage conditions of the adhesive, such as temperature and moisture content, as well as precise geometrical properties of the hole and rods, require special attention to the manufacturing process of these joints. These manufacturing criteria make the application of glued-in rods on the construction-site challenging and thus limit the possibilities of glued-in rods application for renovation of existing structures.

Figure 1.3- Sample of glued-in rods. The rods were inserted along the timber grain.

1.3 MECHANICS OF GLUED-IN RODS

It is crucial to understand the governing mechanisms of the failure of glued-in rods connections. The glued-in rod joint is a hybrid connection, made up of three different materials (wood, adhesive, and rod) with different mechanical properties, which have to work simultaneously. This significantly complicates the analysis of this connection and is also the main reason for lack of full understanding of the behavior of this joint as well as a unified design method. For screws fastened into the timber, the compression between the wood and the sides of the screw leads to the pull-out strength of screws, which is related to the diameter and the anchorage length of screws. Glued-in rod connections with rod diameters very close to the hole diameter, this kind of compression mechanism is very similar. Therefore the load transferring mechanism is affected by the ratio of the rod diameter to the diameter of the hole.

Another mechanism is related to the shear of the adhesive during axial pulling, which leads to the load transmission between timber and the rod. Accordingly, it is logical to say that glued-in rod connections behave as a combination of adhesive and mechanical joints, since they are governed by the compression mechanism between rod and timber and the shear of the adhesive.

1.4 RESEARCH NEED

Considerable research has been done on timber joints with glued-in rods during the past decades. Universal agreement regarding design criteria for these connections, however, has not been reached and more research is needed to propose a general method of evaluating the strength of glued-in rod connections of any given geometry and component's material. Although the basic rules of the glued-in rods mechanical behavior have been defined and design methods have been proposed, the existing knowledge was not deemed sufficient to be adapted into design standards.

1.5 OBJECTIVES OF THE WORK

There is substantial interest in improving design rules of glued-in rods, because these joints offer a series of advantages over mechanical joints, like the ability to transfer higher local stresses, the easiness and quickness of execution in the construction site, an improved protection from fire and a better appearance of the finished joint.

The objective of the study presented herein was to evaluate the influence of the geometric parameters on axial joint capacity. The experimental and numerical investigations focused on defining the capacity of GFRP rod connections in dependence of rod diameter and anchorage length. The secondary objective was to develop a finite element model that will allow for future parameter optimizations and the application of numerical capacity prediction methods.

2. STATE OF THE ART

2.1. INTRODUCTION

Considerable research has been done on glued-in rods during the past two decades and is still on-going [9]. After all, a universal design criterion for timber joints with glued-in rods has not yet been attained. Therefore further studies would help to increase knowledge and experience and contribute to developing a reliable design method.

Glued in rods are used in heavy timber constructions where joints with a large load capacity are needed. Considering the large load requirement and complex load combination, more knowledge was necessary considering safety during design of glued-in rods. So far, tests and research have been carried out by researchers and engineers, and different models and theories have been proposed to characterize the strength of joints [9]. Previews studies theorized that the pull-out strength of joints depends on some geometric parameters (anchorage length, rod diameter, adhesive thickness, etc.) as well as on timber density and moisture content [9].

2.2. MANUFACTURING

A few methods for manufacturing glued-in rods have been described in the literature. In one of these studies, Johansson-Jänkänpää tested the method of horizontally gluing-in of rods [6]. The result was a considerable decrease in the pull-out strength of the joint, because in this method the adhesive could not be allocated uniformly along the anchorage length. However, this effect could not be avoided by fabrication in other positions.

Another method of fabrication, using undersized holes has been applied and tested in Sweden [9]. The manufacturing process included applying adhesive to the hole and rod, and then

screwing the rod into the hole. By using this method the adhesive is better preserved in the hole; the adhesive, however, may not be distributed uniformly along the rod.

Harris (2004) found that the best technique was to inject the resin using an extension on the applicator nozzle and starting at the bottom of the hole allowing the EPX to push the applicator nozzle back out [14]. Once the appropriate amount of EPX has been injected, the rod is inserted. This process pushes out the EPX without introducing air bubbles.

2.3. MECHANICAL PERFORMANCE

The mechanical performance of joints with glued-in rods depends on many parameters such as: geometry of the joint, the materials used, loading conditions and boundary conditions. The influence of a wide range of these parameters has been the subject of many studies conducted during the past researches, leading to the development of design formulas for connections with glued-in rods.

Four primary modes of failure exist for the ultimate limit state:

- Failure of the rods;
- Failure in the adhesive or in its bond to the rod or timber;
- Failure in the timber adjacent to the glue line;
- Failure in timber member in the form of block tear-out.

Each of these failure modes can be analyzed using fundamental engineering design principles and material properties of the rod and timber and, in many cases, material standards are available for the rod and timber. The investigation of the adhesive failure mode, however, is the most complex. Particularly since there is less information available and many different products exist.

To eliminate one of the sources of failure, most design standards do not permit reliance on the bond between the adhesive and the rod.

Bainbridge et al. (2002) performed connection tests to observe the four distinct failure modes through the rods failure, failure in the adhesive (causing breakdown of the material in the bond-line itself), failure in the wood substrate and failure at the interface between timber and adhesive [3]. From the results, it was apparent that that there is sufficient variation in failure modes to confirm that failure may be due to damage in any of the component materials (steel rod, adhesive or timber substrate) or breakdown of the timber to adhesive bond interface.

2.4. ADHESIVES

Different types of adhesives have been used in glued-in rods connections; including phenol-resorcinol, EPX and PUR adhesives. Early work focused on using EPX; in later works, the use of PUR adhesive has increased [9]. Polyurethane adhesives do not depend on moisture for cure, but rely on a hardener, therefore they may be used in place of epoxy resins in many cases because of difficulty to control the moisture content of the wood in construction sites. The choice of the most suitable adhesive depends on the method of fabrication, types of adherents and the gap distance between the rod and the hole, but beyond all these criteria, it should be checked that the adhesive bond will not be the weakest link of the connection.

In the experimental work of the GIROD research project [1], three types of adhesives were tested and compared and it was revealed that the type of adhesive, cause increasing pull-out strength in the following order: phenol-resorcinol (PRF), PUR and EPX.

Bainbridge et al. [3] performed an experimental investigation including duration of load tests involving adhesive bonded rods with three types of adhesive (EPX, PRF and PUR), subject to

high fractions of ultimate load in an outdoor climate, and fatigue studies. Across the studies, the three adhesives behaved in different ways. The key to the adhesive performance and quality is the moisture interaction in the bonding process. Results revealed that the failures at the wood-adhesive interface occurred only in the specimens with PUR adhesive. This is because of CO_2 bubbles at the bond, which cause a reduction in the effective cohesion. Failures within the bond-line were only observed in the samples with PRF adhesive. All samples with EPX had timber related failures result in pull-out of a 1-2 mm plug of wood surrounding the adhesive.

The slight increase in glue-line thickness generally increases failure loads [24]; this is due the increase in the timer-adhesive contact area which in most cases is the dominant failure mode. However, in order to achieve greater contact area between wood and adhesive, instead of increasing the adhesive thickness, it is recommended to increase the rod diameter and keep the adhesive thickness small. This is because of the possibility of adhesive shrinkage while using the large volume of bonding agent. EuroCode 5 also recommends the use of thin adhesive layers [4].

The study of Martitegui et al. [19] showed that the increase in the shear strength of EPX formulations over time is significant. The strength at 1 and 7 days is at least 50% and 80 %, respectively, of the strength at 21 days, and the final strength (at 21 days) is independent of the type of EPX formulation used. The shear strength of the epoxy which is extremely important since the load is transferred from the reinforcement to the member by shear in the adhesive, is about 19 MPa after 21 days which is much higher than that of the wood at 9-12 MPa (coniferous timber). The shear and compression strength of EPX formulations are greater than those of timber, and therefore this material can be used for connection with other materials and to substitute deteriorated timber under compression.

2.5. GLUED-IN FRP RODS

Martitegui et al. [19] evaluated the bonding quality of glued-in rods made with three types of wood; Laricio pine, Radiata pine (higher shear strength) and oak with two kinds of GFRP (plates and rods made with polyester resin reinforced with mat and roving glass fibre) that were glued using three different EPX formulations. EPX adhesive was used, because of its negligible shrinkage while curing and gap filling properties. The bending strength and modulus of elasticity of the EPX formulations were obtained by three point load tests in three 20×20×300 mm specimens according to UNE 56537: 79 [26]. The compression strength was obtained in four 20×20×60 mm specimens according to the UNE 56535: 77 [25]. Both standards are set for small defect-free timber specimens. The bonding shear strength of glued lines was obtained according to ASTM D 905 [27]. This method consists of shear testing glued lines by means of a compression load. The glue types used had modules of elasticity less than the timber. When used in repair however, higher proportion of fillers is added to raise the modulus of elasticity above that of the timber. It is also said that the bending resistance of the glue is not an important factor, since most of the bending stress is taken by the reinforcement. As a result of difference between the properties of the material used in this type of hybrid system and their behavior under different condition, there is a need for a bond that can cope with these issues. One issue is the effect of temperature increase which results in dilation, in the other hand, in wood it causes shrinkage due to loss of moisture.

Regarding the effect of surface treatment, roughness on timber and FRP rods was evaluated and from the results, it was concluded that an unplanned timber surfaces have higher shear strength, while the previous sanding of FRP rods is not advantageous and surface cleaning with solvent is enough.

2.6. SIGNIFICANT RESEARCH PROJECTS

A significant research project, GIROD, was undertaken by the European Union [1]. It was initiated as a large research project on timber joints with glued-in rods in 1998. The objective of the project was to provide the information necessary to prepare design rules for European standards, develop test methods for the evaluation of adhesives and derive production control standards. This project included comprehensive experimental studies and theoretical analysis. The experimental program covered a variety of tests on component materials and also upon bonded rod specimens including axial load tests, transverse load tests, tests on rods at angles to the grain, tests on multiple configurations of rods, ultimate strength tests following various conditioning schedules, duration of load tests in various exposure climates and fatigue tests. These were supposed to lead to the development of a calculation model, tests methods for adhesive and production control standards. The results showed that a calculation model based on Volkersen theory [31] and fracture mechanics provided reasonable prediction of the pull-out strength for glued-in rods bonded with PUR or EPX adhesive.

Broughton and Hutchinson [10] conducted an experimental study on glued-in rod connections. In their tests, holes were filled with adhesive and the rods were inserted slowly in order to avoid the formation of any voids. For moisture content (MC) of 10%, the failure occurred at the adhesive for Sikadur EPX. For the samples glued with Rotafix EPX, the adhesive failure at the rod adhesive interface was the only failure mode observed regardless of the type of wood or bar. Comparing the stress values suggest that Rotafix provided almost exactly the same adhesion to GFRP as it does to steel. For MC of 25% and higher, the failure occurred only in the adhesive with a thin layer of timber. The difference between stress values reached only appears in samples

where the failure has occurred in the timber or timber-adhesive interface where the properties of the timber influence the failure load.

The experimental work of Otero Chans et al. [15] focused on glued-in rods made with threaded steel bars bonded with EPX in hardwood saw timber of high density. The results showed that failure load is not proportional to the anchorage length nor to the rod diameter, which means the failure load is not proportional to the timber-adhesive surface. However, an increase in any of these parameters yields an increase in the failure load. The results also confirmed that a linear relation between timber density and failure load does not exist. Failure of the wood through splitting, failure of the wood-adhesive or a combination of the two was the dominant failure mode. It was observed that the results were not compatible with the values from design formulas.

Otero Chans et al. [16] performed some experiments to assess the effect of timber density on the strength of glued-in rod joints. Two samples of chestnut (medium density, 560 kg/m^3) and tail (high density, 870 kg/m^3) were tested. Prior to testing, the samples were checked for any defects. The tail specimens with highly interlocking grains were found to be more uniform and regular and less defective than the chestnut specimens. Threaded steel rods are mostly preferred over plastic rods or other types of steel rods because of the mechanical interlocking they provide. The load transfer mechanism from the bar to the adhesive in threaded rods is mostly through interlocking; hence surface treatment of the rods is not required. A number of glues were tested and 2-component EPX was found to be the strongest. A number of brand names were tested and for glue line thickness of 1 mm, no major difference was observed. The specimens were tested for pull-out with a constant speed of 0.6-1.2 mm/min. The tests were of short duration taking about 5 minutes. The most common mode of failure was the shear failure of the timber at the

timber-adhesive interface. All of the tail specimens and more than half of the chesnut specimens failed in this manner. The reason that tail specimens failed in the same manners can be attributed to the homogeneity and uniformity in the samples. It was also found that defects in the samples did not influence the failure mode. It was concluded that with increasing anchorage length in the chesnut sample, the number of specimens that failed through the tensile failure of the rods increases. Despite a large difference between the timber densities, the failure loads were very similar; therefore no linear relationship between timber density and joint strength could be established.

The factors determining the durability of structural adhesive joints can be grouped into three categories: environmental (moisture and temperature), materials and the stresses to which the bond is subjected [17]. The environment to which joints are exposed plays an important role in their durability. Test results have shown that glued-in rods lose strength due to exposure to high temperature and humidity over a period of time and in extreme conditions they may collapse. Besides the environmental factors mentioned above, the materials involved in a structural joint also influence bond strength and durability. The factors in the material category include the adherents, the adhesive, wood species, surface preparation and the design of the joint. Finally the means by which the load is transferred, i.e., joint geometry and configurations have been considered as one of the factors determining the durability of these joints.

Otero Chans et al. [18] performed a broad experimental study on joints made with threaded steel rods glued with different types of adhesives and in different hardwood species. Over 400 specimens were tested with different geometric configurations, varying anchorage length, rod diameter and adhesive thickness. This paper presents a summary of the results obtained in the

experimental analysis and proposes a model for predicting joint strength in sawn timber based on shear strength of the wood as a function of joint slenderness.

2.7. NUMERICAL MODELING

Several finite element analyses (FEA) and numerical models have been applied in the past to investigate the performance of glued-in rods in timber structures. An early example of FEA in the modeling of these joints is the work by Muller and Roth [20]. They used a rather coarse finite element mesh to assess the linear elastic stress distribution and its dependence on some geometrical parameters. Later, Aicher et al. presented larger models used for stress distribution analyses and heat transfer modeling [7]. A reasonably more complex numerical model have been developed by Guan, who used a built-in stress-based debonding feature of the finite element code combined with a contact algorithm to model the failure of the adhesive layer and the interaction between the failure surfaces [20]. A nonlinear two-dimensional, axisymmetric model using a bond line model for wood-adhesive bonds was presented by Johansson et al. Here the strain-softening behavior of the bond line was taken into account and the progressive failure of a glued-in rod joint was modeled [6]. The main aim of the numerical simulations was to present new approaches in modeling the pull-out strength of glued-in rods and to indicate what factors might be of interest to include in future design equations.

2.8. DESIGN METHODS

Some of the known design recommendations regarding strength of axially loaded timber joints with glued-in rods are described here; including Riberholt, Gerold, EuroCode 5 and GIROD.

Riberholt

The pioneering work by Riberholt [2] included theoretical and experimental studies, which were carried out to establish general criteria for the design and sizing of these joints. The study focused on the analysis of the strength of joints with glued-in rods in glued laminated timber (glulam). The following design equations were proposed:

$$F_k = f_{ws}\rho_k D\sqrt{l} \quad \text{for} \quad l \geq 200mm \tag{1}$$

$$F_k = f_{wl}\rho_k Dl \quad \text{for} \quad l < 200mm \tag{2}$$

where:

F_k: characteristic failure load of joint;

ρ_k: characteristic density;

D: hole diameter;

l: anchorage length.

The material constant f_{ws} (called also withdrawal parameter for the square root case) and f_{wl} (called also withdrawal parameter for the linear case) are given by $f_{ws} = 650\, N/mm^{1.5}$ and $f_{wl} = 46\, N/mm^2$ for non-brittle glues, e.g. 2-component PUR. For brittle glues, such as resorcinol and EPX $f_{ws} = 520\, N/mm^{1.5}$ and $f_{wl} = 37\, N/mm^2$.

Eqs. (1) and (2) were derived on a purely empirical basis by curve fitting of the experimental results. This result is typical for the design equations found in the literature with the pull-out load given by a nonlinear function of the material and geometrical parameters.

Gerold

Gerold [5] proposed for the calculation for strength of joint to consider the rod slenderness, while keeping material density as one of the design parameters. This is for the reason that the equation both Riberholt and EuroCode 5 proposed, assumed that joint strength depended linearly on the timber/adhesive contact surface area, and the other decisive parameter considered in the formulas was timber density:

$$F_{mean} = \pi \times d \times L \times \left(\frac{\rho_{mean}}{380}\right)^{0.55} \times f_{v,mean} \tag{3}$$

$$f_{v,mean} = 12.6 \times (1 - 0.042 \times \lambda) \tag{4}$$

where:

F_{mean}: mean failure load of joint;

d: bar diameter;

l: anchorage length;

ρ_{mean}: mean characteristic density;

$f_{v,mean}$: mean bond strength referring to a characteristic density of 380 kg/m3;

λ: slenderness ratio l/d with maximum value of 18.

EuroCode 5

After many experimental models for predicting the withdrawal strength of joints made with glued-in rods in any type of timber, initial design criteria for joints made with glued-in rods in timber joints was included in EuroCode 5:

$$F_k = \pi \times d_{eq} \times l \times f_{v,\alpha,k} \tag{5}$$

$$f_{v,90,k} = 12 \times 10^{-3} \times \left(d_{eq}\right)^{-0.2} \times {\rho_k}^{1.5} \tag{6}$$

where:

F_k: characteristic failure load of joint;

d_{eq}: min[D or 1.25 d];

D: hole diameter;

d: bar diameter;

l: anchorage length;

$f_{v,\alpha,k}$: characteristic shear strength of the wood around the hole;

α: angle between the rod and the fiber direction.

<u>GIROD</u>

Analysis of the first GIROD test results revealed the following preliminary mean shear strength design equations for EPX and the type of investigated brittle PUR:

$$f_{v,mean} = \begin{cases} 8.0 \ N/mm^2 \\ 129 D^{-0.52} \lambda^{-0.62} (\rho/480)^{0.45} \end{cases} \tag{7}$$

and for the softening PRF adhesive:

$$f_{v,mean} = \begin{cases} 6.3 \ N/mm^2 \\ 10.3 D^{-0.17} \lambda^{-0.08} (\rho/480)^{0.45} \end{cases} \tag{8}$$

where:

$\lambda = l/D$;

$D - d \leq 2 \ mm$.

The GIROD research project presented a design formula, based on the generalized Volkersen theory. This calculation model was used as a basis for a code proposal in Eurocode 5. In order to simplify the expressions, it was decided to use the formula for the pull-compression load case, which is an approximation on the safe side. Thus, the pull-out strength is given by:

$$\frac{P_u}{\pi d l} = \tau_f \frac{\tan \omega}{\omega} \tag{9}$$

where:

P_u: characteristic pull − out strength of a single rod;

$\pi d l$: area of the bond;

τ_f: local bond line shear strength;

$$\omega = \sqrt{\frac{l_{geo}}{l_m}} \tag{10}$$

In equation (10), l_{geo} is a geometrical length parameter and l_m is a material length parameter (a measure of the ductility of the bond line), and they are defined as:

$$l_{geo} = \frac{\pi d l^2}{2}\left(\frac{1}{A_r} + \frac{E_r/E_w}{A_w}\right) \tag{11}$$

$$l_m = \frac{E_R G_f}{{\tau_f}^2} \tag{12}$$

The proposal is appropriate for adhesives that develop adhesion to the wood and also to the rod and gives accurate predictions for the pull-compression loading case, and safe predictions for the pull-out loadings.

3. EXPERIMENTAL WORK

3.1. SPECIMEN DESCRIPTION

For all test samples, the same cross sections of timber specimens were adopted (89 by 89 mm). A blind hole was made in each end of the test samples with an intermediate separation (*Li*) equal to the anchorage length (*L*). The lengths of the rods were equal to anchorage length plus 120 mm for griping to the testing machine (*Le*). Details are shown in Figure 3.1.

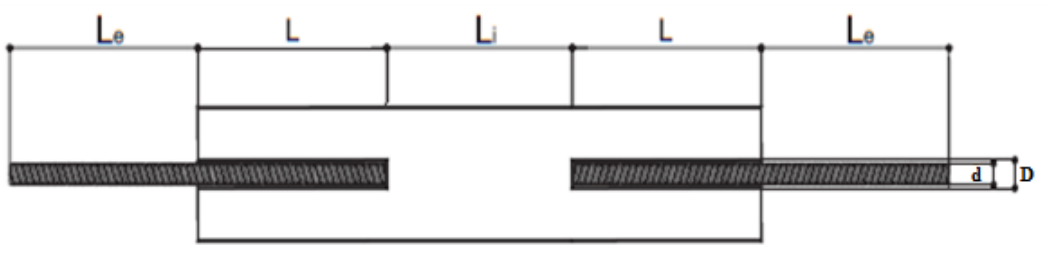

Figure 3.1- Specimen configuration

Five different anchorage lengths (*L*: 50, 100, 150, 200 and 250 mm) were tested for five different rod diameters (*d*: 2/8, 3/8, 4/8, 5/8 and 6/8 in) for a total of 125 specimens. Each type of specimens was labeled with a letter and number as listed in Table 3.1.

Table 3.1-Dimensional characteristics of the samples tested

Series	d (in)	D (in)	L (mm)	Timber dimensions (mm)
A1	2/8	3/8	50	89×89×150
A2	2/8	3/8	100	89×89×150
A3	2/8	3/8	150	89×89×150
A4	2/8	3/8	200	89×89×150
A5	2/8	3/8	250	89×89×150
B1	3/8	1/2	50	89×89×300
B2	3/8	1/2	100	89×89×300
B3	3/8	1/2	150	89×89×300
B4	3/8	1/2	200	89×89×300
B5	3/8	1/2	250	89×89×300
C1	1/2	5/8	50	89×89×450
C2	1/2	5/8	100	89×89×450
C3	1/2	5/8	150	89×89×450
C4	1/2	5/8	200	89×89×450
C5	1/2	5/8	250	89×89×450
D1	5/8	3/4	50	89×89×600
D2	5/8	3/4	100	89×89×600
D3	5/8	3/4	150	89×89×600
D4	5/8	3/4	200	89×89×600
D5	5/8	3/4	250	89×89×600
E1	3/4	7/8	50	89×89×750
E2	3/4	7/8	100	89×89×750
E3	3/4	7/8	150	89×89×750
E4	3/4	7/8	200	89×89×750
E5	3/4	7/8	250	89×89×750

3.2. MATERIALS

The pull-out strength of glued-in rods is related to the adhesive type, but also the used wood species, since different wood specimens may develop different bonding strength with different adhesives. However, in this study, where the influence of geometrical parameters is of interest, the wood species and adhesive were not variables in the tests.

Douglas-fir Glulam with 89 by 89 mm cross-section was used. The density of 50 randomly selected samples was determined prior to drilling them; the average density of the wood specimens was 562 kg/m^3. The timber moisture content was estimated before every test by a moisture meter at three points along the specimens, as shown in Figure 3.2. Results of average MC measurements for each series of specimens are listed in Table 3.2.

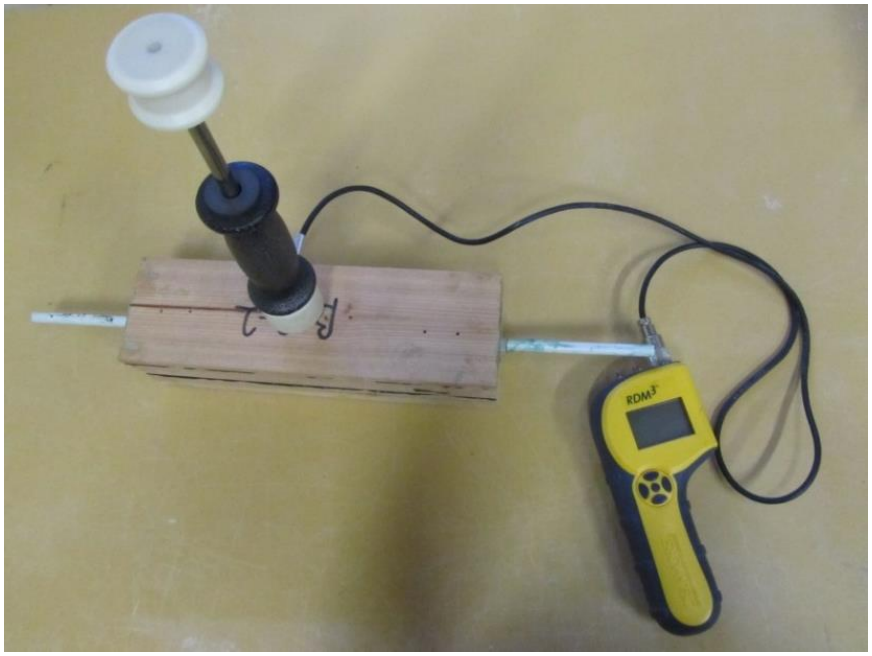

Figure 3.2- Measuring of moisture content by moisture meter

Glass fibre reinforced polymer (GFRP) material (manufactured by Bedford Reinforced Plastics) was used as rod for the specimens. These materials perform well in terms of ease of

manufacturing, light weight and statically efficient connections. The tensile strength of the GFRP rods was determined to 468.7 MPa and the elastic modulus to 35.0 GPa by means of tensile tests on the same material as used for the joint specimens. The diameter of the rods were 2/8, 3/8, 4/8, 5/8 and 6/8 in, respectively, see Figure 3.3.

In order to prepare the rods, they were cut into small pieces for different anchorage length, and then sanded in order to get better adhesion. Particular attention was devoted to the cleaning of the rods surface with solvent and of the hole with an air blow gun to remove dust in order to optimize the strength of the joints.

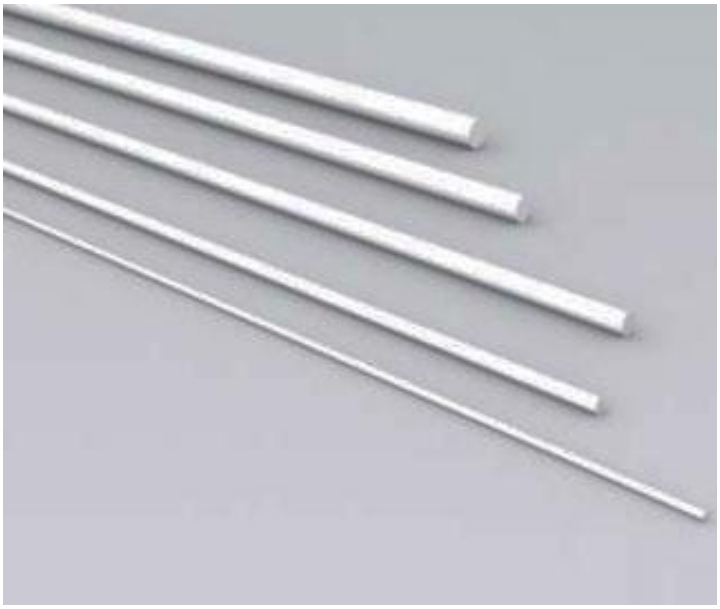

Figure 3.3- FRP rods with different diameters

The used adhesive was a two-component injectable polyurethane adhesive (PLIOGRIP 7779), manufactured by Valvoline. PLIOGRIP PUR adhesives do have gap filling capability, and while they do not carry structural ratings, are used for structural bonding of composite plastics and coated metals in automotive and industrial applications.

3.3. SPECIMEN MANUFACTURING

With respect to the geometric configuration of the test specimens, the thickness of the adhesive was fixed to 1/16 in. It is crucial to use proper thickness of the adhesive, since larger thickness might develop shrinkage that will cause significant stresses in the joint.

The holes were made with a diameter 1/8 in larger than the rod diameter; therefore to center the bar in the hole a suitable foam tape was used at the end of the rod which was inside the hole. The full cartridge of structural adhesive was installed into the injection gun (Figure 3.5). The rear end of the cartridge was placed vertically and centrally over the holes and the adhesive was injected into the base of the holes up to approximately 1/3 of the length of the holes.

Figure 3.4- The adhesive cartridge gun and nozzle for gluing 2-componnent PUR adhesive

Then the rods were glued into the predrilled holes, parallel to the grain of timber, under continuous pressure (Figure 3.5). The GFRP rods were inserted into the samples with a twisting action, allowing even distribution of the adhesive around the rods.

Figure 3.5- Specimens and rods are prepared for gluing procedure

The distances of the rods from the edge of the timber were taken into consideration to avoid splitting failure of the timber. Since if the edge distance is too small, splitting failure will occur, but it was not the case in this experimental study.

3.4. METHODS

Pull-pull tests were performed, as a tension force was applied to the rod at both sides of the samples. The samples were tested until failure in a universal testing machine INSTRON 8802 with load capacity of 250 kN. Load and displacement values were recorded. Displacements were recorded by using Linear Variable Differential Transformers (LVDTs). The specimens were tested until failure by applying loads under displacement control at a rate of 2.5 mm/min assuring that all the test samples failed in a time of 5 ± 2 min. Figure 3.6 shows the pull-out test set up.

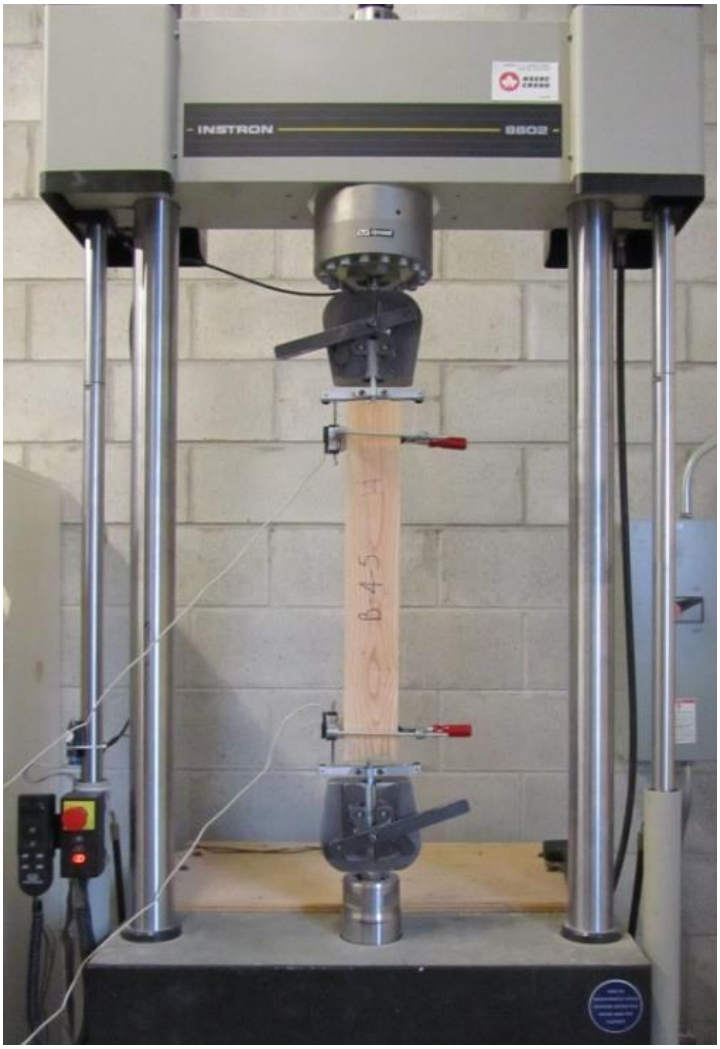

Figure 3.6- Machine and testing device of the samples

3.5. RESULTS

For every specimen, a data file was obtained that registered the load applied to the test sample, the relative displacement of the cross-head and the displacement data from two LVDT devices. Table 3.2 summarizes the failure load mean values and Standard Deviations (StDev) of all test series, average relative displacement of the side that failed and the average MCs. All individual specimen results are listed in Appendix A.

Table 3.2- Results obtained in the tests

Series	Average MC (%)	Failure load (kN)		Average relative displacement (mm)
		Average	StDev	
A1	10.7	6.4	0.4	0.4
A2	11.0	13.4	1.6	0.8
A3	10.9	15.0	0.9	0.9
A4	11.2	17.3	0.7	1.0
A5	10.4	18.3	1.4	1.1
B1	12.1	10.9	1.3	0.5
B2	10.8	18.9	2.0	0.9
B3	10.8	19.8	2.6	1.0
B4	10.6	25.0	1.8	1.1
B5	11.6	25.7	2.2	1.2
C1	10.5	14.2	1.9	0.5
C2	10.4	22.1	3.5	0.8
C3	10.8	26.6	2.7	1.0
C4	11.2	32.9	1.6	1.1
C5	11.5	34.7	1.8	1.2
D1	10.8	17.6	1.8	0.5
D2	11.1	29.1	3.5	0.9
D3	10.7	46.6	2.9	1.4
D4	11.0	52.1	6.6	1.5
D5	11.4	54.4	6.3	1.6
E1	9.8	19.3	1.9	0.5
E2	10.6	40.8	1.8	1.0
E3	10.5	47.6	2.8	1.2
E4	11.4	58.5	3.9	1.4
E5	10.6	66.7	2.8	1.6

3.6. ANALYSIS OF EXPERIMENTAL RESULTS

The two parameters analyzed were the rod diameter and anchorage length on the joint strength. First the failure load values for specimens with constant anchorage length but with varying rod diameters were compared and then the failure load values versus anchorage length were compared, as respectively shown in Figure 3.7 and Figure 3.8.

First, the influence of the diameter of the rod was studied. For this step; the graph of the failure load versus rod diameter was obtained and the values of failure load for the specimens with a same anchorage length, but with different rod diameter, were compared (Figure 3.7). It is observed that, in all the cases, when increasing the diameter of the rod, the value of the failure load increases. It would be possible to conclude that this increase in the value of failure load was related to the increase in the surface between the timber and the adhesive. The values of failure load in Table 3.2 show that the relationship between this surface and the load capacity of the joint is not linear. With greater diameters, the increase that takes place in the failure load is greater in test samples with a greater anchorage length.

For the next step, the graph of the failure load versus anchorage length was obtained and the values of failure load for the specimens with a same rod diameter were compared (Figure 3.8). The results show that increasing the anchorage length increases the failure load of the specimens. Nevertheless, the obtained increase of load is not proportional to the increase of the anchorage length. When the values corresponding to the test samples with smaller anchorage lengths are compared, the obtained increase in load is approximately proportional to the increase in the anchorage length. But this is not the case for longer anchorage lengths. The reason is that the shear stress distribution in the timber-adhesive interface is more uniform in shorter anchorage lengths.

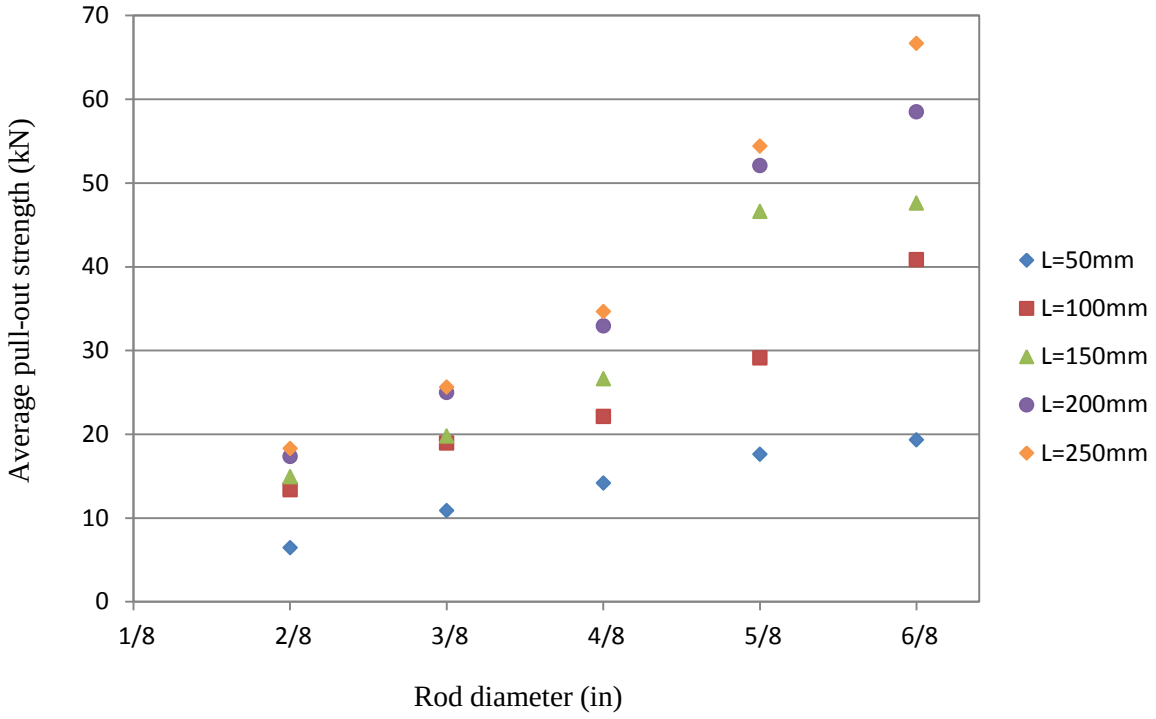

Figure 3.7- Average failure loads of specimens for different rod diameter

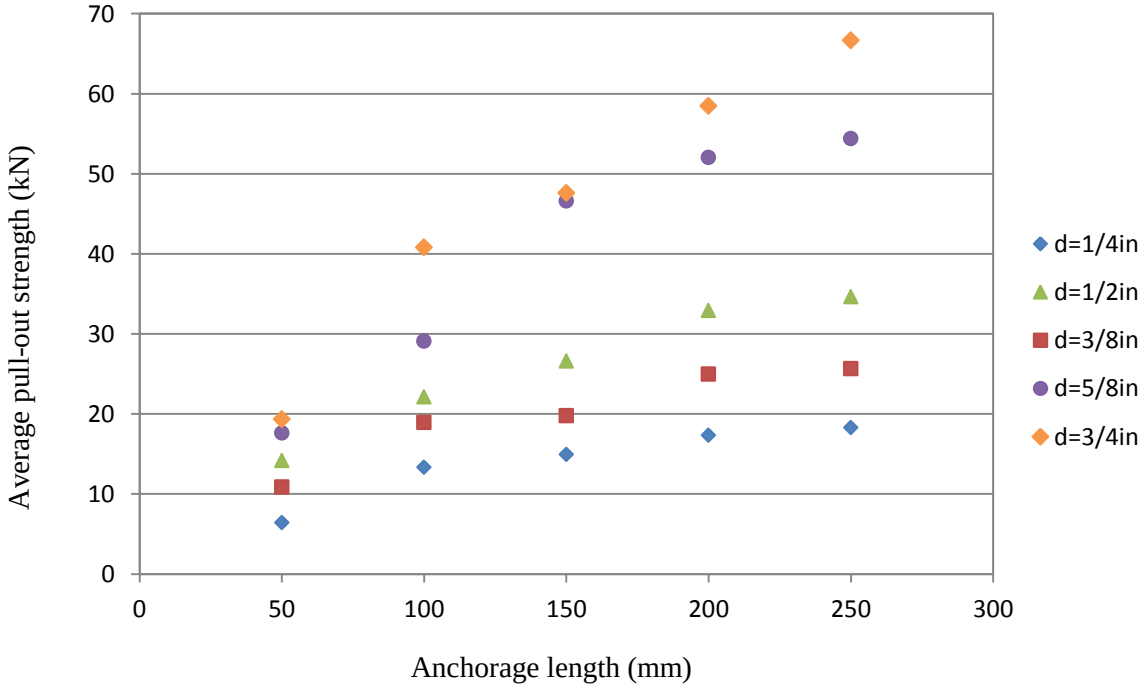

Figure 3.8- Average failure loads of specimens for different anchorage length

The comparison of the load-displacement curves for different rod diameters indicates that joint stiffness is directly related to rod diameter. The joints made with thicker rods have higher stiffness. An example of this behavior is shown in Figure 3.9 for load-displacement curves corresponding to an anchorage length of 150 mm. The load-displacement curves for all series of test specimens are shown in Appendix A (Figure A. 1 to Figure A. 5).

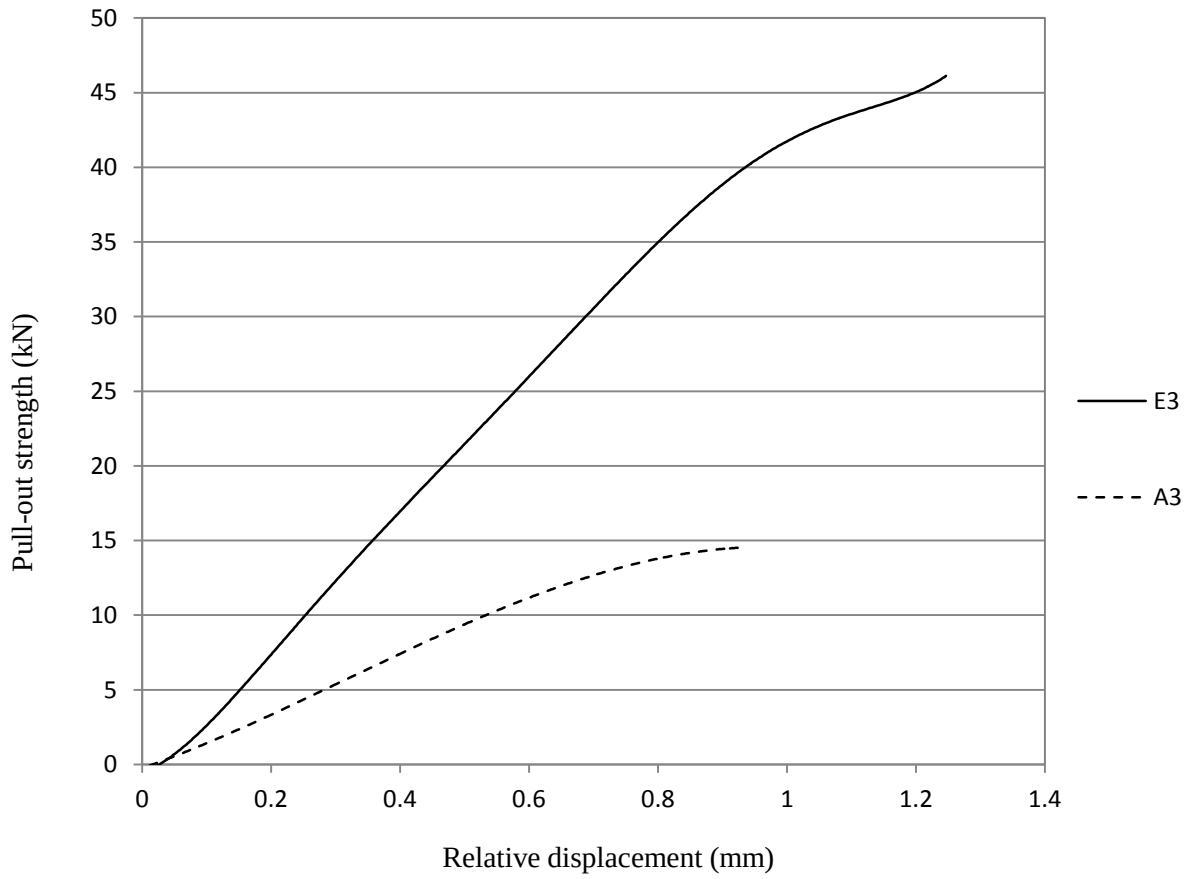

Figure 3.9- Load-displacement curves for specimens with 150 mm anchorage length

The software package SAS 9.3 [21] was applied for the statistical analysis of experimental data. The type of test was two factor factorial experiment and treatments were the combinations of two factors and there were five levels of rod diameter (factor A) and five levels of anchorage length (factor B). All levels of factor A occur for factor B and vice versa (factorial experiment or

crossed treatments), therefore 25 treatments were generated. Considering five replications per treatment, there were a total of 125 experimental units. Treatments randomly assigned to the 125 experimental units (test specimens) and the measured response was pull-out strength of glued-in rods.

Analysis of variance (ANOVA) was carried out to evaluate the effect of anchorage length and rod diameter on the joint strength. P-values were calculated and compared to the significance level, α, herein chosen as 0.05 which is a typical value. If the p-value is smaller than α, the null hypothesis of no differences between means is very unlikely, and thus rejected. This procedure was applied and the ANOVA table showing the sources (main effects and interactions) and degrees of freedom for each source is laid out in Table 3.3.

Table 3.3- Analysis of variance

Source	Degrees of freedom	Mean Square	F-stat	p-value
A	4	4183.49	540.68	<0.0001
B	4	2628.07	339.66	<0.0001
A × B	16	192.05	24.82	<0.0001
Total (including error term)	121			

One purpose of this study was to determine whether there was a relationship (a) between the levels of rod diameter and pull-out strength and (b) between the levels of anchorage length and pull-out strength of glued-in rods. Results were analyzed by using a factorial ANOVA with two between-subjects factors. This analysis revealed a significant main effect for both rod diameter and anchorage length in the prediction of the joint strength (Table 3.3).

Another purpose of this study was to determine whether there was a significant interaction between the levels of rod diameter and the levels of anchorage length and pull-out strength of the joints. Results were analyzed by using a factorial ANOVA with two between-subjects factors. This analysis revealed a significant statistics for the interaction between the levels of rod diameter and the levels of anchorage length ($p<0.0001$). According to a significance level of 5% ($\alpha=0.05$), the A×B interaction is significant. This indicates that in the population, there is an interaction between the levels of rod diameter and the levels of anchorage length in the prediction of the criterion variable (pull-out strength of the joints).

The effect of MC on strength of glued-in rods joint was investigated using the analysis of covariance (ANCOVA). ANCOVA helps to explain the variability in the response variable due to changes in continuous explanatory variables (called covariates). In this experimental design, the MC and density are two covariates that their possible effects on pull-out strength of glued-in rods were investigated. The analysis showed changes in MC does not significantly affect the pull-out strength.

Similar to MC, investigation on the effect of density on joint strength was done and no correlation between the density of the test samples and the critical load was found (Table 3.4). It should be noted that in both cases the coefficient of variation were too small (especially for density), which might affect this finding.

Table 3.4- Analysis of covariance

Source	Degrees of freedom	CV (%)	Mean Square	F-stat	p-value
MC	121	8	28.13	1.30	0.17
Density	46	3	269.68	1.81	0.35

3.7. ANALYSIS OF SECOND (UNBROKEN) JOINT

Maximum Likelihood Method (MLM) provides estimation for parameters of a statistical model. MLM uses s mathematical expression known as the likelihood function of the data to describe a set of unobservable data [29] [30]. MLM was applied to the series of test specimens that had identical joints at both ends. Since joints were symmetrically designed at both ends and only the weaker side failed, the resulting data were censored. It also provided the information that the pull-out strength of the other side is higher.

Considering *n* test specimens of glued-in rods, a series of *n* observations for joint strength was obtained $(x_1, x_2, \dots, x_n)$, which follows a probability density function with the parameter θ (Eq. (13)) :

$$L_1 = \prod_{i=1}^{k} f(x_i|\theta) \tag{13}$$

For the other end of the specimens (unbroken end), the probability function can be defined by a random variable X and using the information that strength values are larger than the survivor ends (Eq. (14)) :

$$L_2 = \prod_{i=1}^{n} P(X \geq x_i|\theta) \tag{14}$$

with $P(X \geq x_i|\theta) = 1 - f(x_i|\theta)$ (15)

Because of the wide application of the Weibull distribution in life-testing and time to failure distributions, the two-parameter Weibull distribution have been used to model the strength probability distribution of glued-in rods. Then the method of censored maximum likelihood has been applied using these two likelihood functions (Eqs. (13) and (14)) to estimate model's parameters.

Five samples with 150 mm anchorage length and 0.5 in rod diameter were considered to illustrate the censored MLM. The results showed that the cumulative distribution function (CDF) fitted to the data by Censored MLM differs significantly from the CDF of the sample data (Figure 3.10). According to the 5th percentile values of their CDF, this amount differs by 5 to 10% for different series. The CDF curves for all series of test specimens are shown in Appendix A (Figure A. 6 to Figure A. 10).

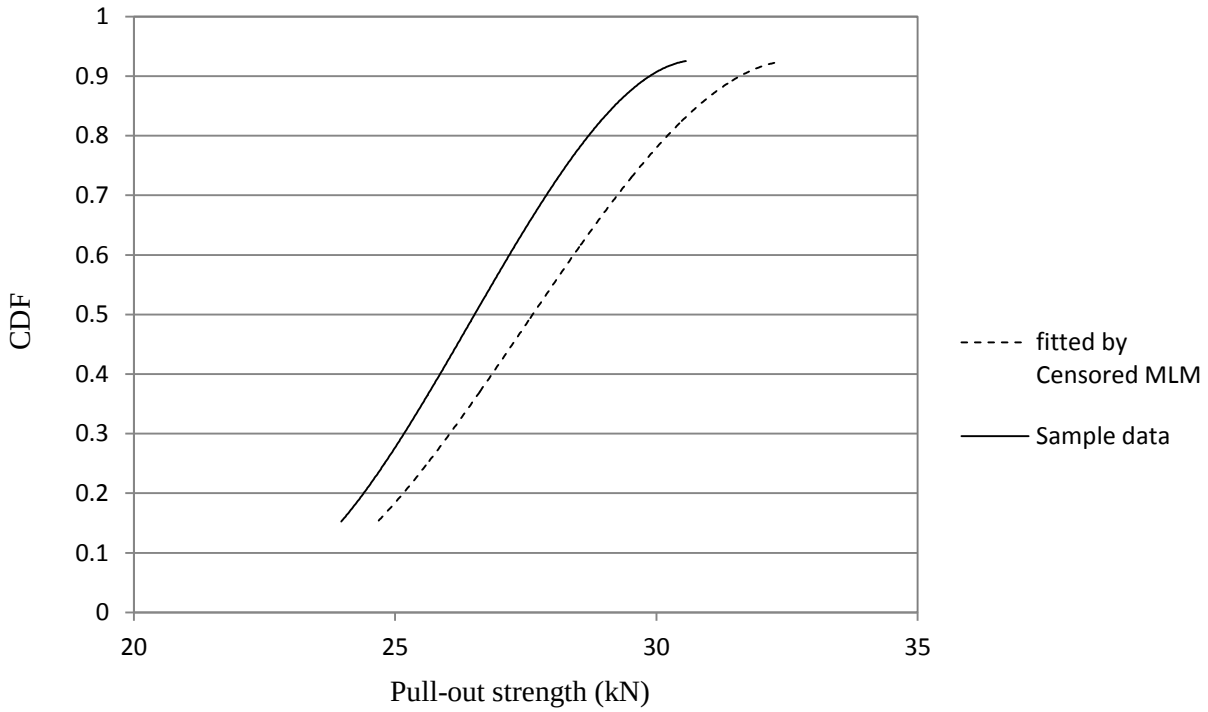

Figure 3.10- CDF with parameters estimated using sample data and censored MLM

3.8. COMPARISON WITH DESIGN METHOD PREDICTIONS

The experimental failure loads have been compared to the theoretical values provided by the eqs. (1) to (5) included in the literature review. In all cases the experimental results were lower than the theoretical values (Figure 3.11 to Figure 3.14).

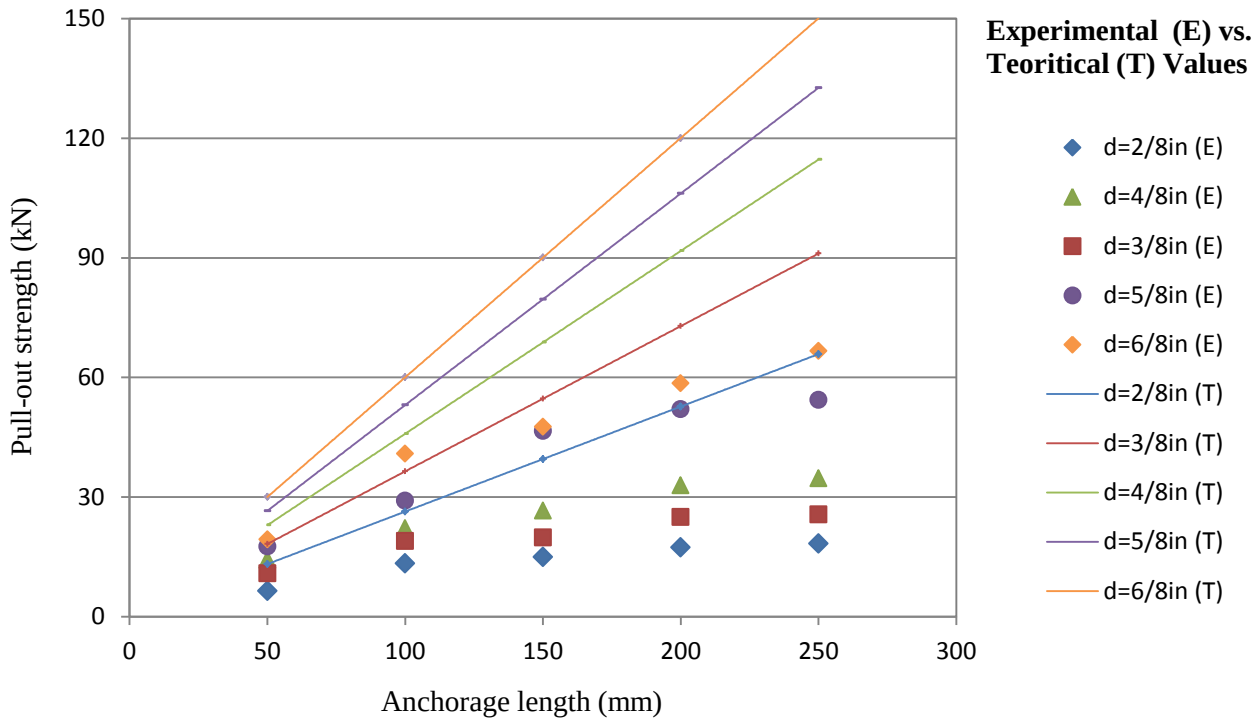

Figure 3.11- Experimental data vs. design value from eq. (1) and (2), Riberholt

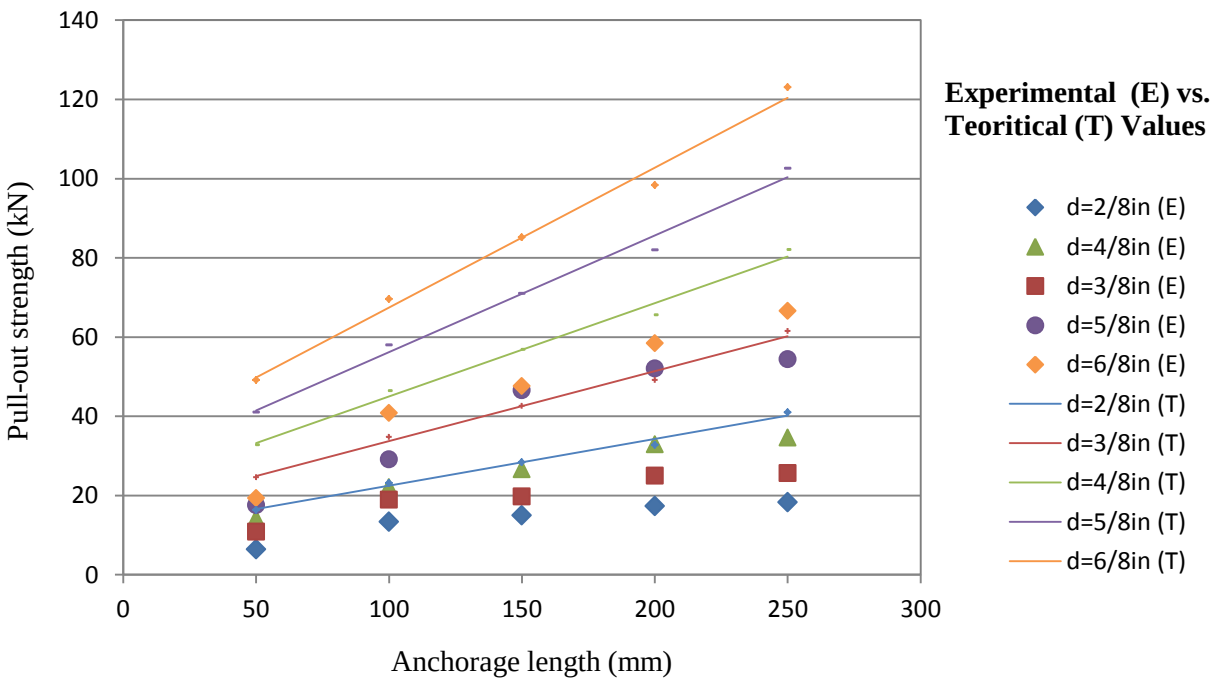

Figure 3.12- Experimental data vs. design value from eq. (3), Gerold

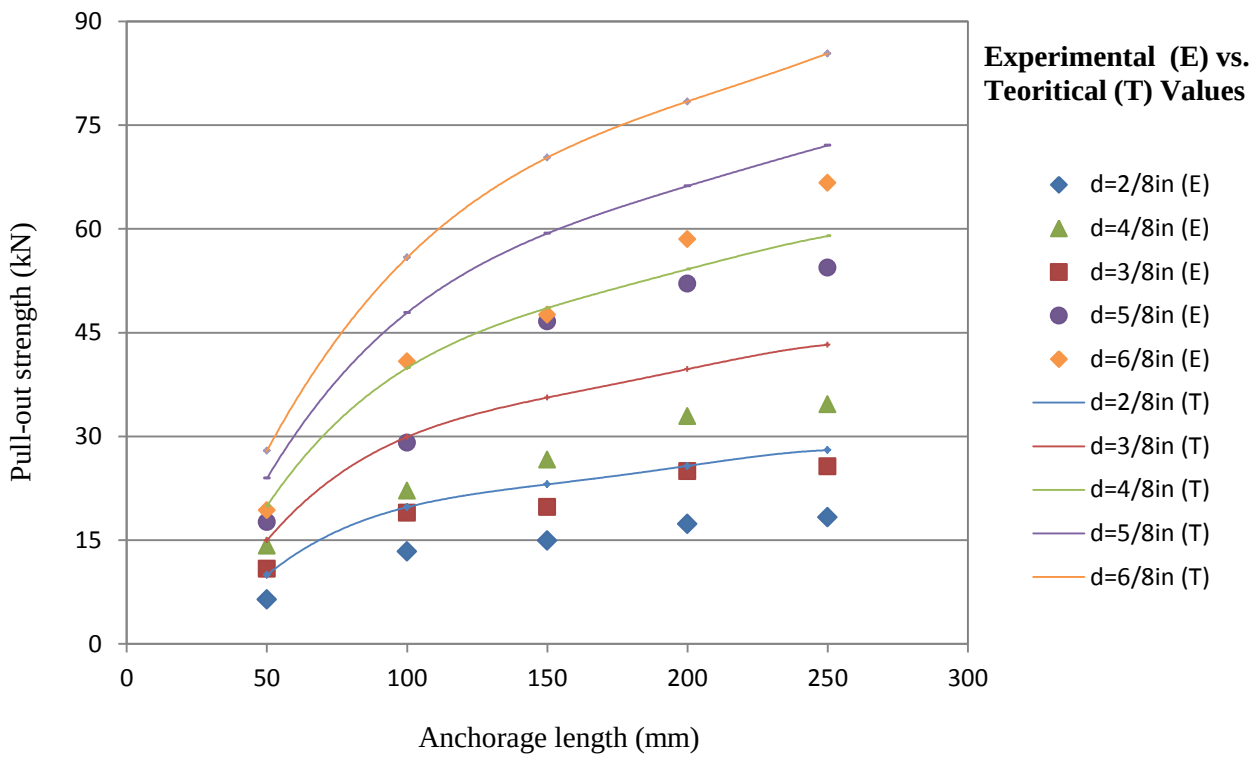

Figure 3.13- Experiment data vs. design value from eq. (5), EuroCode 5

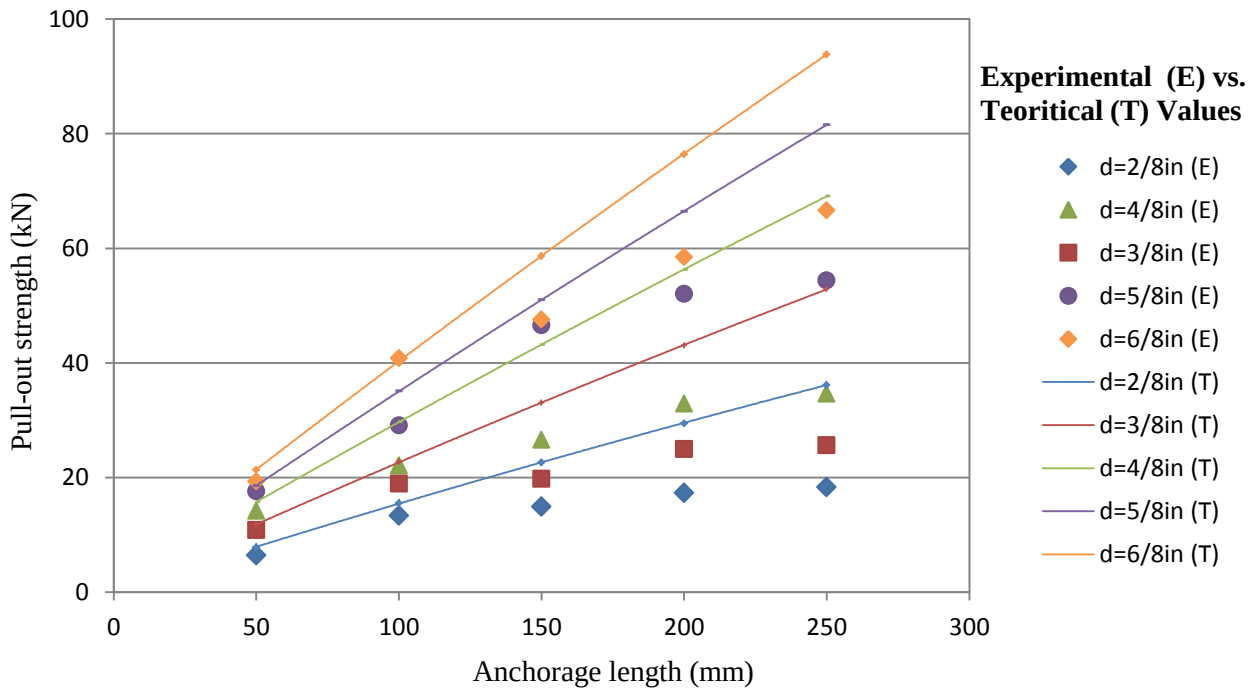

Figure 3.14- Experiment data vs. design value from eq. (8), GIROD

To investigate the goodness of fit for design equations, the graphs of the predicted versus measured strength values were interpreted; the results indicates that the experimental loads were lower than the design predictions by 40% in average. The coefficient of multiple determination (R^2) is a measure that commonly used to indicates how well the curve fits the data, which normally ranges from zero (very poor) to one (perfect fit). The R^2 values for three design equations were calculated and it was observed that all R^2 values were negative. The reason is that the corresponding outcomes have been derived from the design equations and not a model fitting procedure. It also indicates that the error in the prediction exceeds standard deviation in sample data, and the mean of the data provides a better fit to the outcomes rather than the design equations values.

3.9. DISCUSSION

The experimental study on glued-in rods has emphasized significant difference in the strength of these joints compared to the predictions of different design methods; however the overall effect of geometrical characteristics on the joint strength has been confirmed, which shows the axial strength of the joint is not linearly proportional to the timber-adhesive interface.

In most of the cases, the failure took place by shear at the interface between adhesive and timber and the extraction of the bar was accompanied by timber fibres (Figure 3.15), or a small timber block (Figure 3.16); which demonstrated that the failure had taken place in the timber and not in the adhesive joint. However for some samples with smaller rod diameter the mode of failure with yielding of the rod was observed (Figure 3.17).

Considering the most frequent failure mode (shear failure of wood along the rod), it can be concluded that the strength of timber joints with glued-in rods is basically related to the surface area of the anchoring zone and on the shear strength of the wood-adhesive interface.

Figure 3.15- Mode of failure related to shear failure of wood along the rod (Rod completely pulled out for investigation)

Figure 3.16- Mode of failure in which the rod was extracted with a small timber block

Figure 3.17- Mode of failure with fracturing of the rod

Previous research [23] showed that the edge distance has to be at least equal to 2.5 times the bar diameter in order to avoid splitting failure, however experimental tests presented in this research showed that an edge distance equal to 2 times the bar diameter could also avoid splitting failure.

Moreover, based on the obtained load-displacement curves, the joints made with thinner rods have lower stiffness. This can be an important aspect to consider in the design of timber joints with glued-in rods that should not have a fragile failure under cycling loads.

4. NUMERICAL ANALYSIS

4.1. MODEL DEVELOPMENT

To characterise the stress distribution within timber connections with glued-in rods, a 3D FEA model was developed using the commercial software package ANSYS 14.0 [22]. The kind of joint geometry used and element subdivision studied are shown in Figure 4.1 and Figure 4.2. Due to symmetry only one half of the length of the specimen as well as one quarter of the cross section of the specimen were modelled, which leads to reduce computation time. The coordinate system has been defined in which the origin of the coordinates fixed at the centre of the rod on top of the joint and Z axis located longitudinally along the rod.

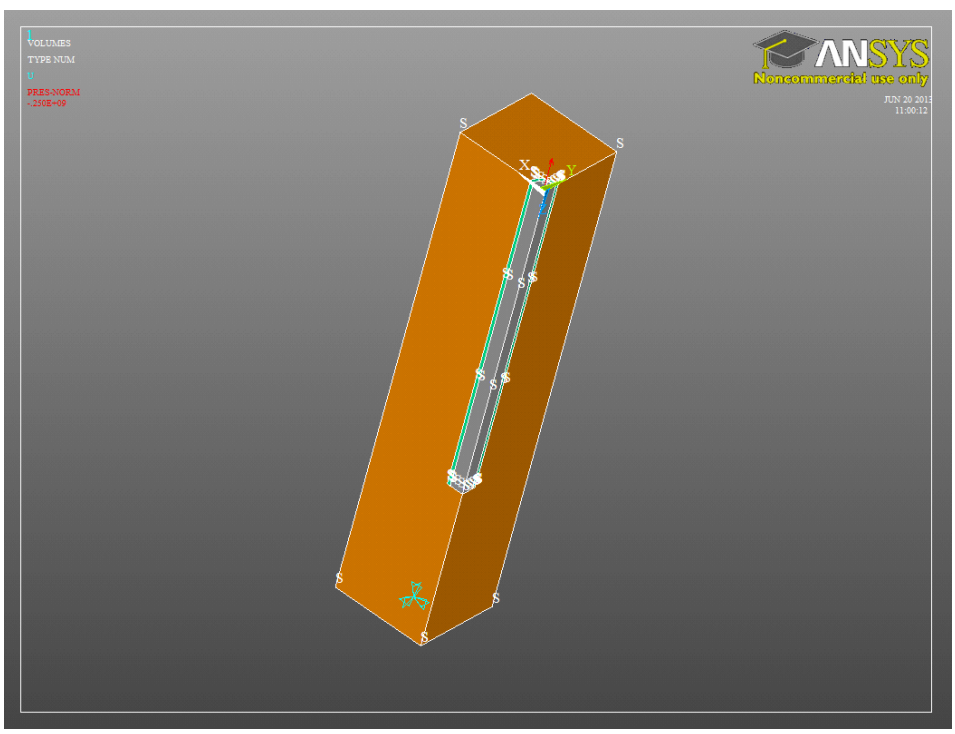

Figure 4.1- The finite element model of the glued-in rod joint.

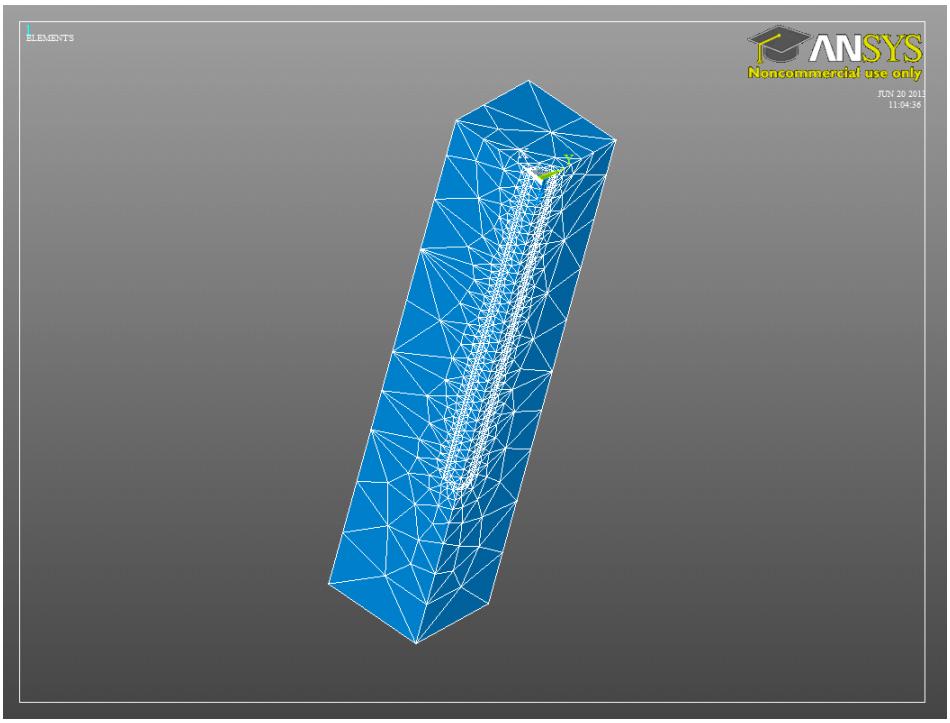

Figure 4.2- FE-mesh: The finest mesh was used in zones of high stresses.

SOLID186, a higher order three dimensional, 20-node solid elements have been used that exhibits quadratic displacement behavior. This means that the element is defined by 20 nodes having three degrees of freedom per node. The element supports plasticity, hyperelasticity, creep, stress stiffening, large deflection, and large strain capabilities. It also has mixed formulation capability for simulating deformations of nearly incompressible elastoplastic materials, and fully incompressible hyperelastic materials.

The wood material has been modelled as being a linear elastic orthotropic material. The influence of the actual annual ring curvature of the timber was found to have a negligible effect on the results, and therefore the material directions were assumed to be constant along the specimens. The numerical values of the elastic parameters of wood that have been used in the model are given in Table 4.1. The GFRP rods and PUR adhesives were modeled as being linear elastic and isotropic with the mechanical properties laid out in Table 4.1.

Table 4.1- Material properties in the FEA model

	Elastic modulus (GPa)		Poisson's ratio		Shear modulus (GPa)	
Wood	E_X	0.5	ν_{XY}	0.38	G_{XY}	0.07
	E_Y	0.5	ν_{YZ}	0.02	G_{YZ}	0.7
	E_Z	10.0	ν_{XZ}	0.02	G_{XZ}	0.7
GFRP rod	E	35.0	ν	0.27	G	25.0
PUR adhesive	E	1.5	ν	0.40	G	2.5

To model the contact between timber and the rod, surface to surface contact technology has been used. This type of contact provides linear traction-separation, standard contact behavior after debonding and capability with unloading and reloading. For bonded contact, Contact Manager can be used to define areas of bonded contact for delamination and then assigning Material ID to contact pair. Normal penalty stiffness (FKP), penetration tolerance (FTOL) and friction coefficient (μ) are the parameters of surface to surface contact, which affect model accuracy and convergence. These coefficients have been chosen based on previous experience and values reported in the literature. FKP constant was set herein to 2×10^{10}, FTOL to 0.5 and μ to 0.9, which led to convergence and realistic interpenetration of the surfaces.

All degrees of freedom were constrained for the base surface of the specimen and the pull-out load was applied as pressure on the top surface of the rod. All types of specimens have been modeled and for each test series the average failure load was applied to the model. The applied load and constraints are shown in the Figure 4.1.

4.2. COMPUTED ROD DISPLACEMENTS

Figure 4.3 shows a displacement plot of series C3. It can clearly be seen that most of displacement in the system occurred in the rod and its surrounding. These results are in

coincidence with the experimental observations, which in most of the cases the failure occurred by shear at the timber-adhesive interface and the extraction of the rod was accompanied by wood fibres.

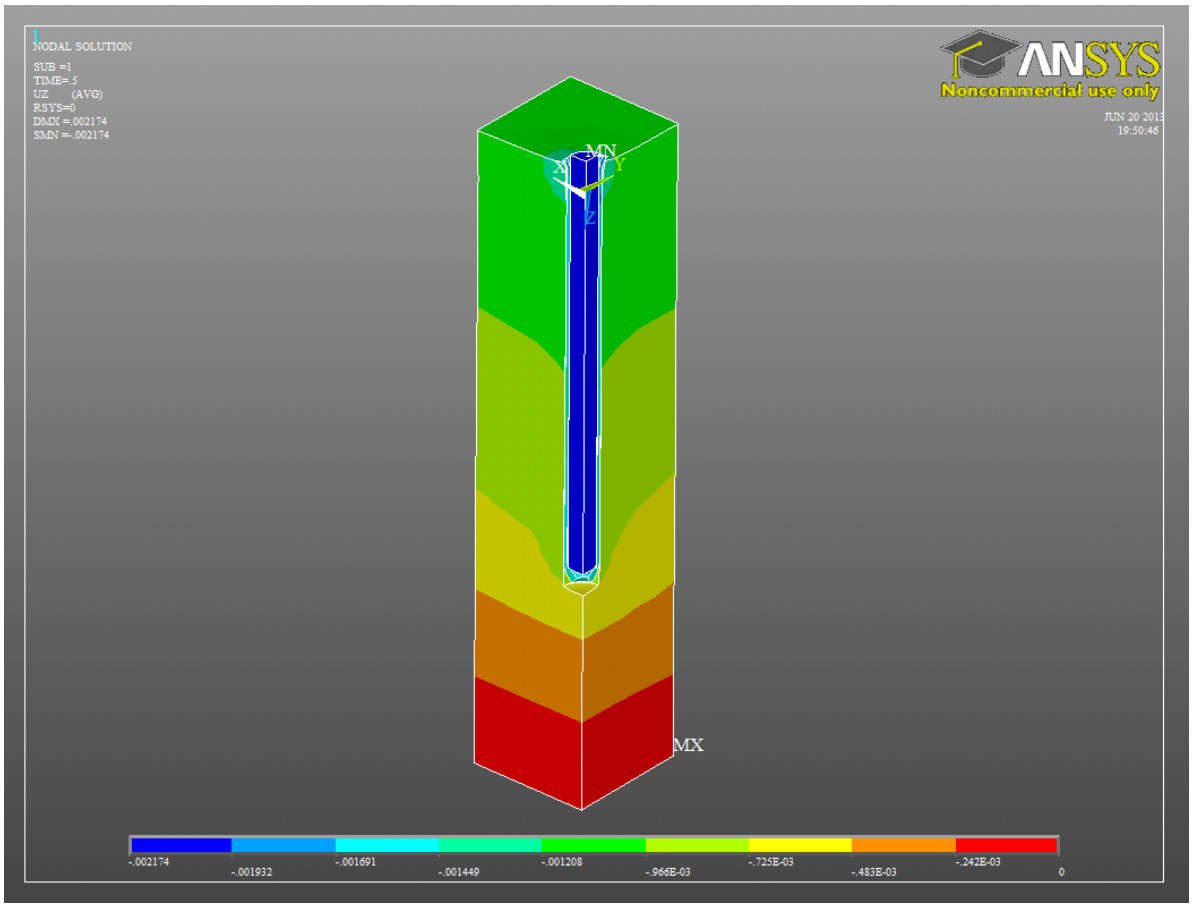

Figure 4.3- Computed displacement in vertical (Z) direction

The load-displacement response curves obtained from numerical simulation and experimental analysis illustrated in Figure 4.4. From the following mentioned results, it can be concluded that the experimental results were confirmed by numerical model with respect to overall deformation. Therefore the model is reliable in predicting the structural response of glued-in rods, however the model and experimental curves have different shapes. The load-displacement curves for all models are shown in Appendix C (Figure C. 1 to Figure C. 24).

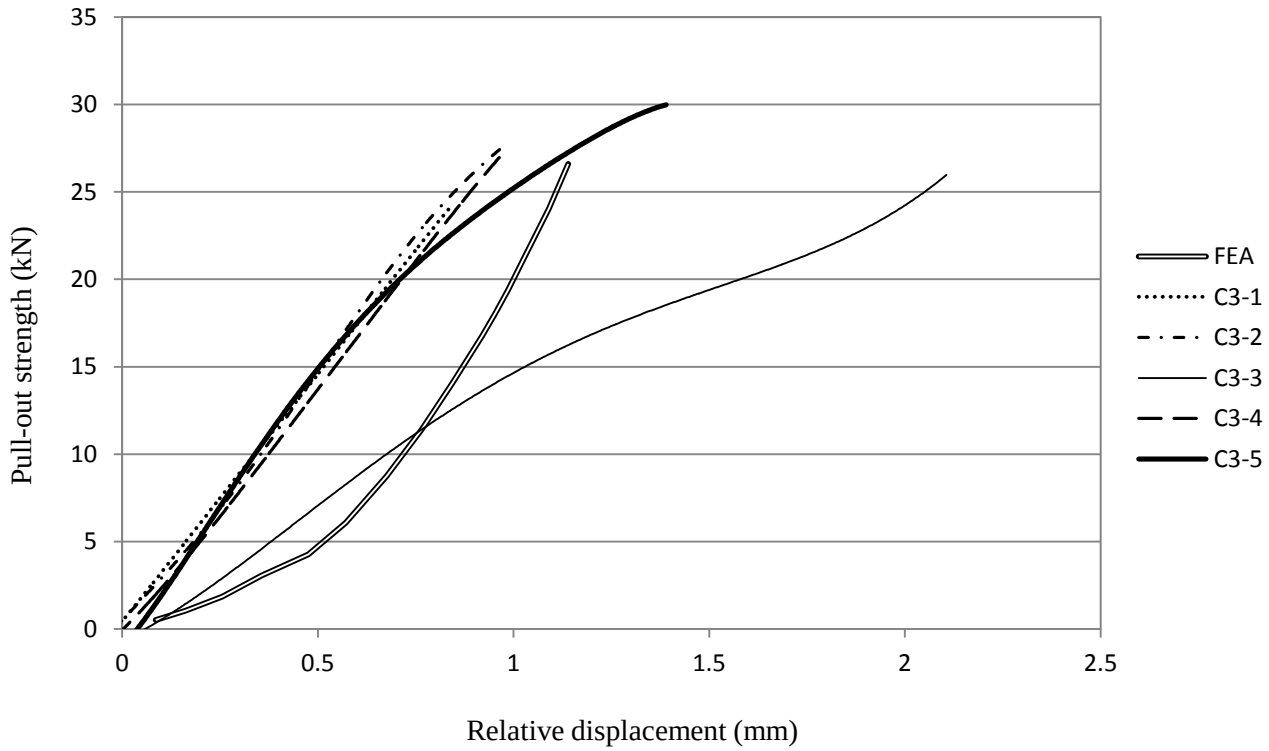

Figure 4.4- Load-displacement curves from experimental tests and FEA for specimen of type C3

4.3. STRESS DISTRUBUTION ALONG ANCHORAGE LENGTH

The distribution of stresses in the joint was computed for series C3 and the contact area at the end and top of the rod was clearly identified as the location of highest stresses. It is also illustrated that as further we go from the timber-adhesive interface, the distribution of shear and tensile stress parallel to grain, become more even and stress peak points at ends of the anchorage disappear gradually (Figure 4.5 and Figure 4.6).

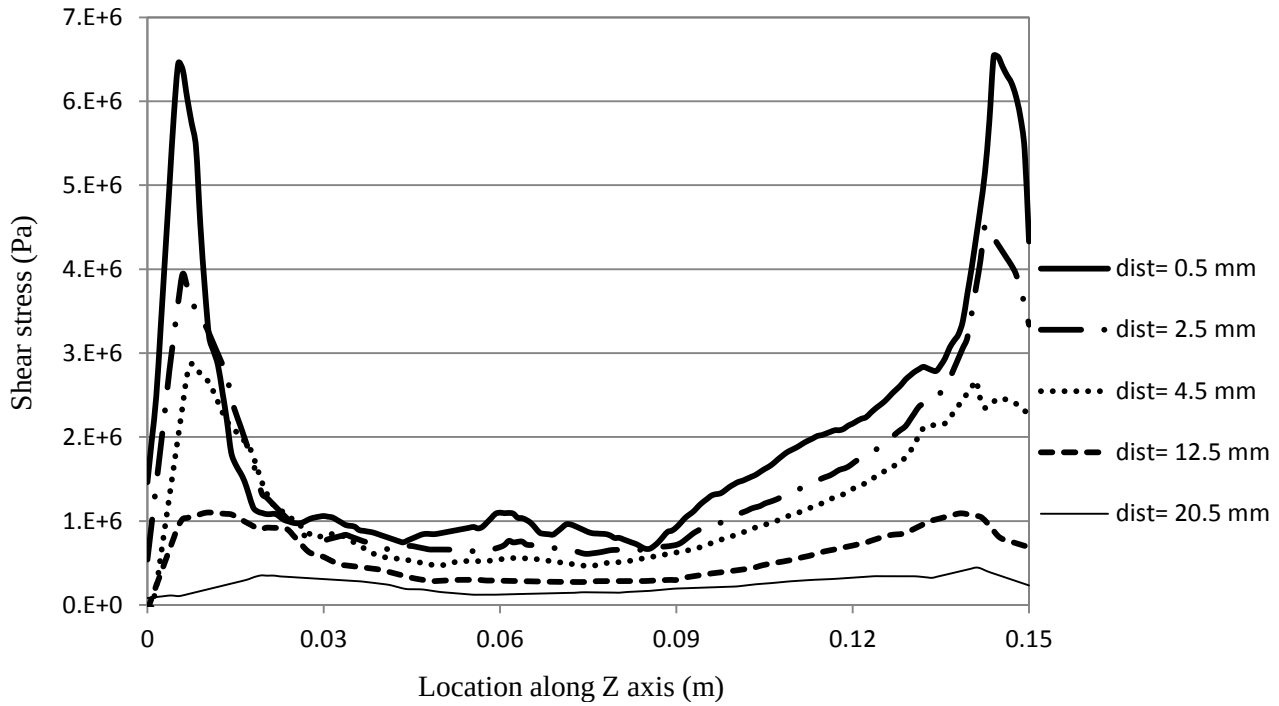

Figure 4.5- Shear stress along the bond-line located at different distances from the bond-line (from dist= 0.5 mm to dist= 20.5 mm)

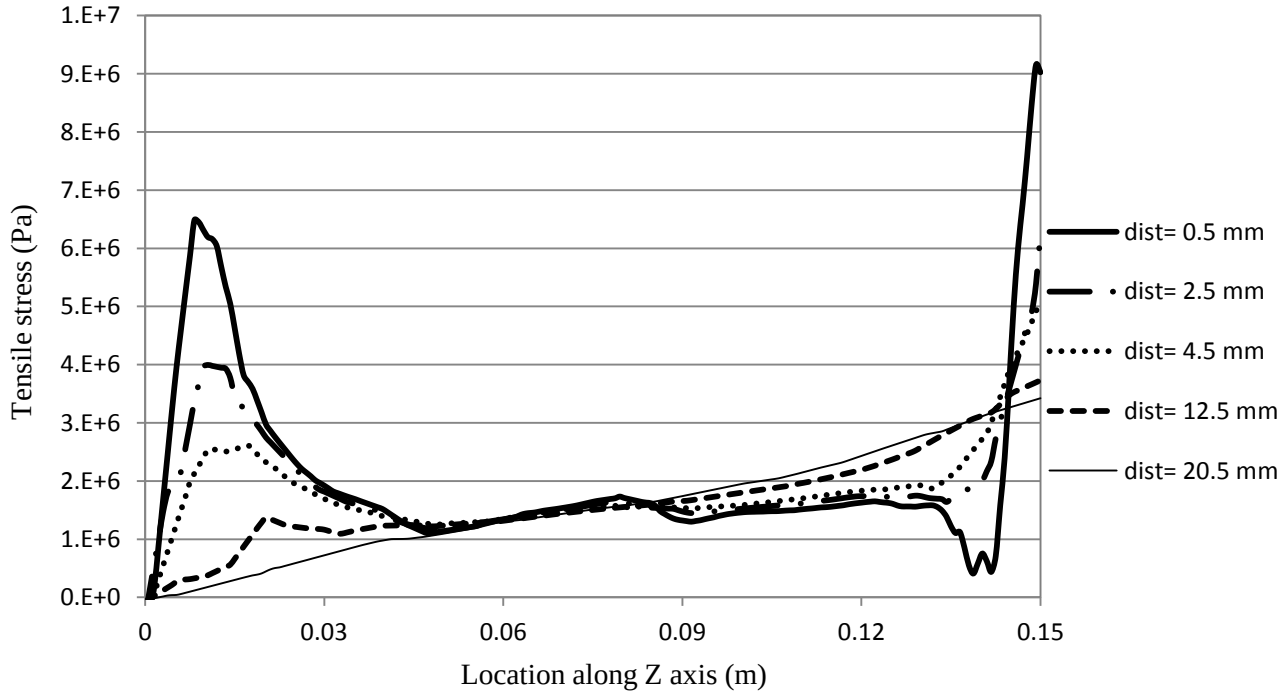

Figure 4.6- Tensile stress parallel to the grain along the bond-line located at different distances from the bond-line (from dist= 0.5 mm to dist= 20.5 mm)

4.4. DISCUSSION

In order to simulate the behavior of timber joints with glued-in rods, a nonlinear, three-dimensional bond-line model was developed by finite element analysis.

The finite element analysis confirmed that the experimentally observed failure location is also the highest stressed part of the model. Also the shear stress plots (Figure 4.5) shows that the highest stress value is very close to the shear strength of Douglas-fir parallel to grain (6.2 MPa) [28]. In addition comparing load-displacement curves from numerical and experimental results revealed that the numerical model accurately reflects the experimentally observed behavior (Figure 4.4). According to these findings, it can be concluded that the model is an effective tools in predicting the structural response of the glued-in rods; including stress distribution, deformation, failure location and failure mode.

5. CONCLUSIONS

Experimental and numerical studies on the influence of geometric characteristics on the structural performance of timber joints with glued-in rods have been performed.

The experimental study focused on joints made with GFRP rods glued with PUR adhesive into the Glulam specimens of Douglas-fir species. A total of 125 specimens were prepared with different geometric characteristics of anchorage length and rod diameter. The specimens then were tested under uniaxial tension load until failure.

The experimental results show that the failure load is not proportional to the anchorage length nor to the rod diameter. This means the joint strength is not proportional to the surface area between the wood and the adhesive. However the statistical analysis revealed a significant effect for both rod diameter and anchorage length in joint strength. The effects of MC and density on pull-out strength of glued-in rods were investigated using ANCOVA, and it was revealed that in the range of variation observed in this study, there was no correlation between these factors and failure load.

Since joints were symmetrically designed at both ends and strength data of unbroken end are censored, Maximum Likelihood Method has been applied to describe these set of unobservable data. This statistical method led to the new cumulative distribution function (CDF) which differs significantly from the CDF of the sample data.

When compared to the predictions of existing design equations for glued-in rods, the experimental failure loads results were lower than the theoretical values in all the cases. Although this might be because of the combination of adhesive and GFRP rod, this conflict

demonstrates the need to review the design criteria of glued-in rods, especially for joints made with FRP rods.

The numerical simulation of glued-in rods joint has been performed using the ANSYS 14.0 software package. The comparison of numerical with experimental results indicated that the numerical model is effective and reliable in prediction of structural behavior of these joints; including stress distribution, deformation, failure location and failure mode.

In the present study the pull-out strength of glued-in rods with single GFRP rods and PUR adhesive was investigated. This work has highlighted significant difference in the strength of these joints compared to theoretical values from different design methods; however the overall effect of geometrical properties on the strength has been confirmed.

It would be beneficial using the numerical results to apply probabilistic capacity prediction method for the joints studied herein. The duration of load, fatigue behavior, bending strength of glued-in rods and joints with multiple rods are the areas where the future experimental investigations would add to the knowledge of these systems and expand the scope of resolvable issues in their design.

REFERENCES

[1] Bengtsson, C., & Johansson, C. J. (Eds.). (2002). GIROD: Glued in Rods for Timber Structures. Sveriges provnings-och forskningsinstitut (SP).

[2] Riberholt, H. (1988, August). Glued bolts in glulam-Proposals for CIB code. In Proceeding of 21th CIB-W 18 meeting.

[3] Bainbridge, R., Mettem, C., Harvey, K., & Ansell, M. (2002). Bonded-in rod connections for timber structures—development of design methods and test observations. International journal of adhesion and adhesives, 22(1), 47-59.

[4] Eurocode 5-CEN/TC 250/SC5 (2004). Design of timber structures. Part 1.1. General - Common rules and rules for building. Final draft EN 1995-1-1.

[5] Gerold, M. (1992). Verbund von Holz und Gewindestangen aus Stahl.Bautechnik, 69(4), 167-178.

[6] JohanssonJänkänpää, L. (2008). Limmade förband i stora träkonstruktioner.

[7] Aicher, S., Gustafsson, P. J., & Wolf, M. (1999, September). Load displacement and bond strength of glued-in rods in timber influenced by adhesive, wood density, rod slenderness and diameter. In First RILEM Symposium on Timber Engineering (pp. 369-378). RILEM Publications SARL.

[8] Jensen, J. L., Nakatani, M., Quenneville, P., & Walford, B. (2011). A simple unified model for withdrawal of lag screws and glued-in rods. European Journal of Wood and Wood Products, 69(4), 537-544.

[9] Tlustochowicz, G., Serrano, E., & Steiger, R. (2011). State-of-the-art review on timber connections with glued-in steel rods. Materials and structures, 44(5), 997-1020.

[10] Broughton, J. G., & Hutchinson, A. R. (2001). Adhesive systems for structural connections in timber. International journal of adhesion and adhesives, 21(3), 177-186.

[11] Broughton, J. G., & Hutchinson, A. R. (2001). Effect of timber moisture content on bonded-in rods. Construction and Building Materials, 15(1), 17-25.

[12] Wiktor, R. (1994). Glulam Connections Using Epoxy Glued-in Rebars (Doctoral dissertation, University of British Columbia).

[13] Micelli, F., Scialpi, V., & La Tegola, A. (2005). Flexural reinforcement of glulam timber beams and joints with carbon fiber-reinforced polymer rods. Journal of Composites for Construction, 9(4), 337-347.

[14] Kashiwagi, T., Harris Jr, R. H., Zhang, X., Briber, R. M., Cipriano, B. H., Raghavan, S. R., ... & Shields, J. R. (2004). Flame retardant mechanism of polyamide 6–clay nanocomposites. Polymer, 45(3), 881-891.

[15] Otero Chans, D., J. Estévez Cimadevila, and E. Martín Gutiérrez. "Glued joints in hardwood timber." International Journal of Adhesion and Adhesives 28, no. 8 (2008): 457-463.

[16] Chans, D. O., Cimadevila, J. E., & Gutiérrez, E. M. (2009). Influence of the geometric and material characteristics on the strength of glued joints made in chestnut timber. Materials & Design, 30(4), 1325-1332.

[17] Custódio, J., Broughton, J., & Cruz, H. (2009). A review of factors influencing the durability of structural bonded timber joints. International journal of adhesion and adhesives, 29(2), 173-185.

[18] Otero Chans, D., Cimadevila, J. E., & Gutiérrez, E. M. (2010). Model for predicting the axial strength of joints made with glued-in rods in sawn timber. Construction and Building Materials, 24(9), 1773-1778.

[19] Arriaga Martitegui, F., Iñiguez Gonzalez, G., & Esteban Herrero, M. (2011). Bonding shear strength in timber and GFRP glued with epoxy adhesives. Wood Research,56(3), 297-310.

[20] Serrano, E. (2001). Glued-in rods for timber structures—a 3D model and finite element parameter studies. International journal of adhesion and adhesives, 21(2), 115-127.

[21] SAS 9.3. Copyright 2002-2010 by SAS Institute Inc., Cary, NC, USA.

[22] ANSYS 14.0. Copyright 2011 SAS IP, Inc.

[23] Blass, H. J., & Laskewitz, B. (1999). Effect of spacing and edge distance on the axial strength of glued-in rods. In Proceedings of the CIB-W18 Meeting Thirty-Two, Graz, Austria, Paper (pp. 32-7).

[24] Bengtsson, C., & Johansson, C. J. (2000). Test methods for glued-in rods for timber structures. In Proceedings of the CIB-W18 Meeting Thirty-Three, Delft, The Netherlands, Paper (pp. 33-7).

[25] UNE 56535, 1977: Physical and mechanical properties of wood. Determination of compression parallel to the grain strength.

[26] UNE 56537, 1979: Physical and mechanical properties of wood. Determination of bending strength.

[27] ASTM D 905, 2008: Standard test method for strength properties of adhesive bonds in shear by compression loading.

[28] Bergman, R., Cai, Z., Carll, C. G., Clausen, C. A., Dietenberger, M. A., Falk, R. H., ... & Zelinka, S. L. (2010). Wood handbook: Wood as an engineering material. Forest Products Laboratory.

[29] Steiger, R., & Köhler, J. (2005). Analysis of censored data—examples in timber engineering research. In Proceedings of CIB W (Vol. 18).

[30] Havbro Faber, M., Köhler, J., & Dalsgaard Sorensen, J. (2004). Probabilistic modeling of graded timber material properties. Structural safety, 26(3), 295-309.

[31] Volkersen, O. (1938). Die Nietkraftverteilung in zugbeanspruchten Nietverbindungen mit konstanten Laschenquerschnitten. Luftfahrtforschung,15(1/2), 41-47.

[32] Volkersen, O. (1953). Die Schubkraftverteilung in Leim-, Niet-und Bolzenverbindungen. Energie und Technik, 5(68), 103.

Appendix A. SUPPORTING DATA

Table A. 1- Failure load for all 5 replicates of each test series

Series	Rod diameter d (in)	Glued-in length L (mm)	Failure load (kN), replicate No 1	2	3	4	5
A1	2/8	50	6.2	6.5	6.0	6.4	7.1
A2	2/8	100	11.1	14.6	12.6	15.0	13.4
A3	2/8	150	16.0	14.4	13.7	15.0	15.7
A4	2/8	200	16.1	17.9	17.2	17.7	17.7
A5	2/8	250	19.8	18.4	18.3	19.0	16.1
B1	3/8	50	9.1	10.5	12.6	11.8	10.3
B2	3/8	100	15.9	19.4	18.3	19.6	21.5
B3	3/8	150	16.3	18.2	20.1	22.4	22.0
B4	3/8	200	22.1	26.0	24.7	25.1	27.1
B5	3/8	250	22.3	25.6	25.5	26.3	28.5
C1	1/2	50	12.1	15.6	14.8	16.2	12.2
C2	1/2	100	25.6	22.6	18.0	19.1	25.4
C3	1/2	150	24.0	27.4	24.3	26.8	30.6
C4	1/2	200	33.1	32.5	30.4	34.4	34.3
C5	1/2	250	32.4	33.4	37.1	35.5	35.0
D1	5/8	50	15.2	19.6	17.5	19.2	16.6
D2	5/8	100	34.9	28.1	29.9	26.3	26.4
D3	5/8	150	49.0	43.1	43.8	49.3	47.8
D4	5/8	200	49.4	44.7	62.2	50.1	54.0
D5	5/8	250	49.2	51.5	53.2	63.6	
E1	3/4	50	19.1	16.3	20.6	21.1	19.5
E2	3/4	100	39.8	41.9	42.6	41.8	38.1
E3	3/4	150	48.1	46.8	51.1	44.4	
E4	3/4	200	58.3	58.0	52.6	63.3	60.2
E5	3/4	250	65.0	68.7	63.6	69.4	

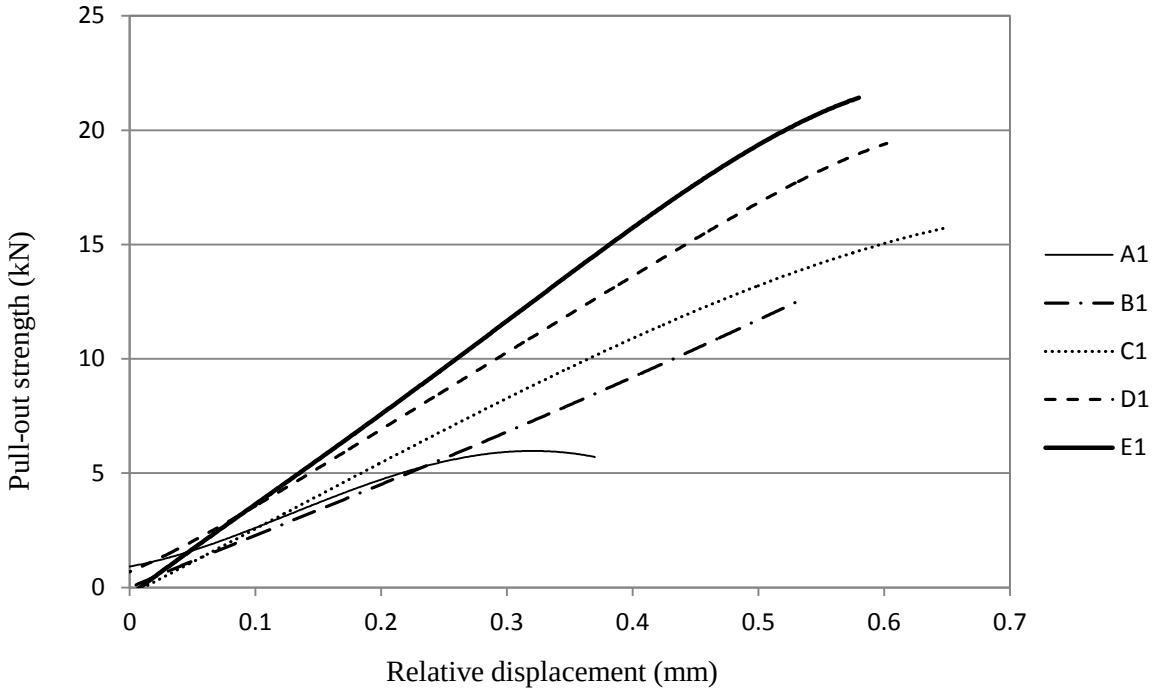

Figure A. 1- Average load-displacement curves for specimens with 1/4 in rod diameter

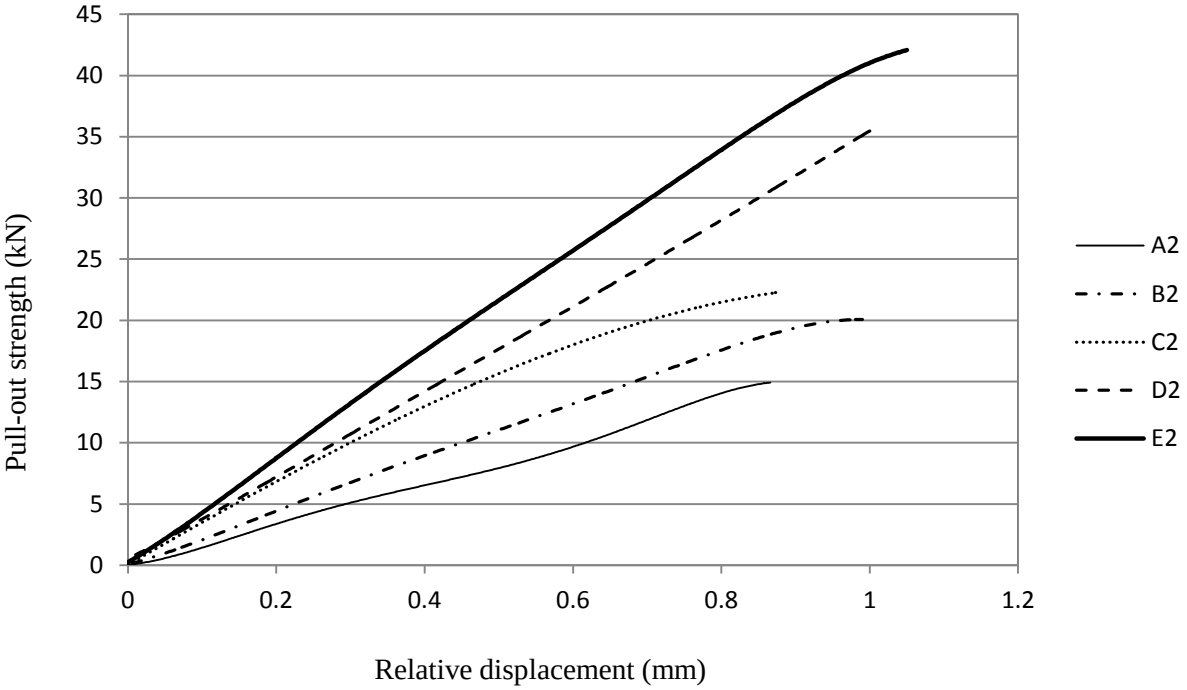

Figure A. 2- Average load-displacement curves for specimens with 3/8 in rod diameter

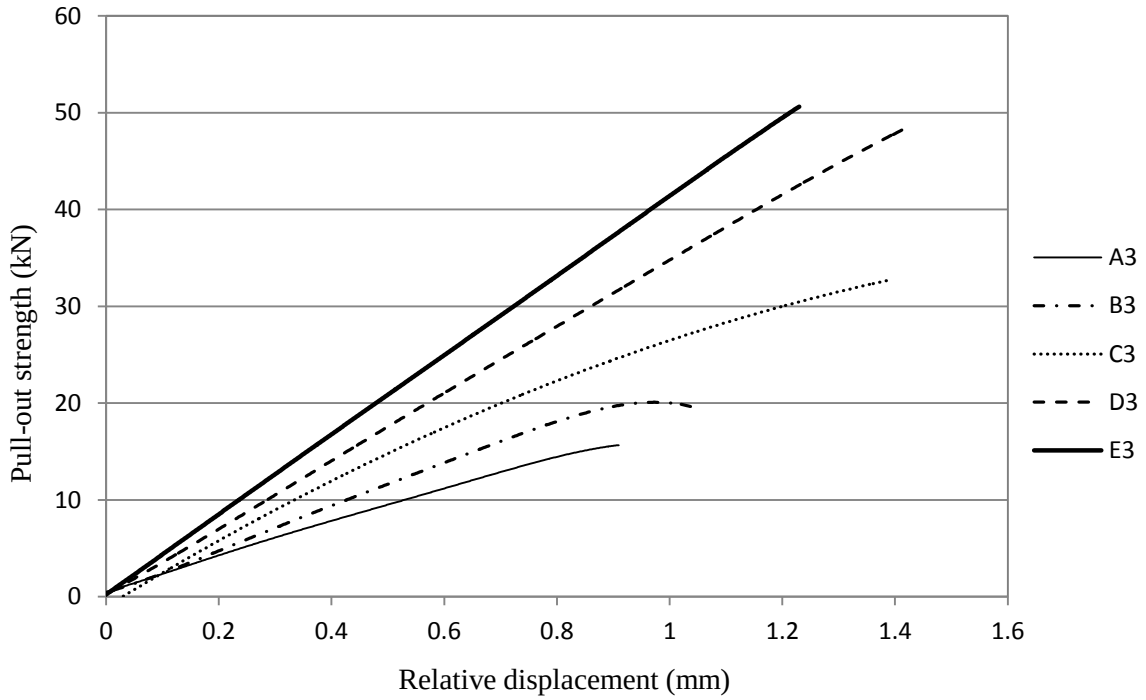

Figure A. 3- Average load-displacement curves for specimens with 1/2 in rod diameter

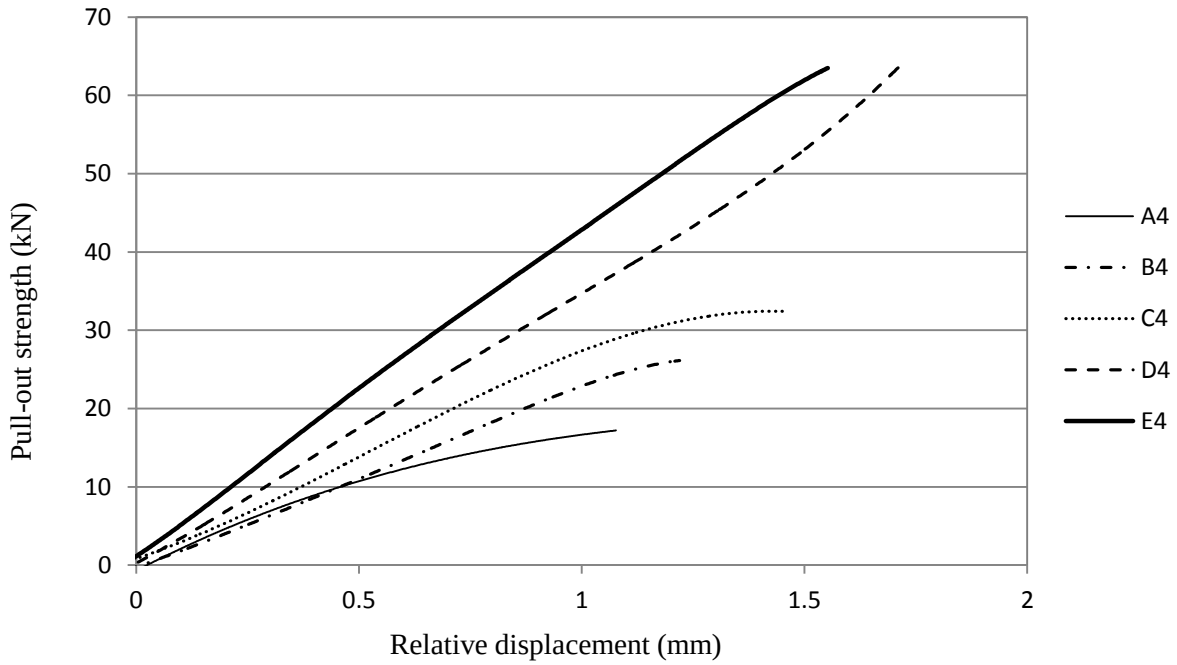

Figure A. 4- Average load-displacement curves for specimens with 5/8 in rod diameter

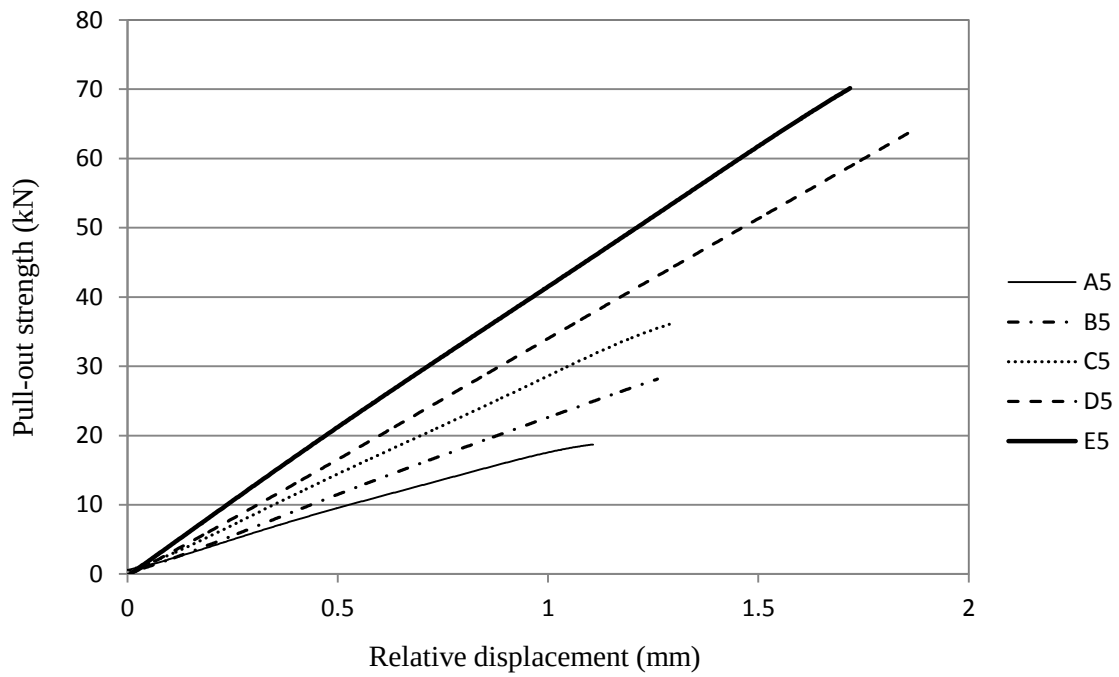

Figure A. 5- Average load-displacement curves for specimens with 3/4 in rod diameter

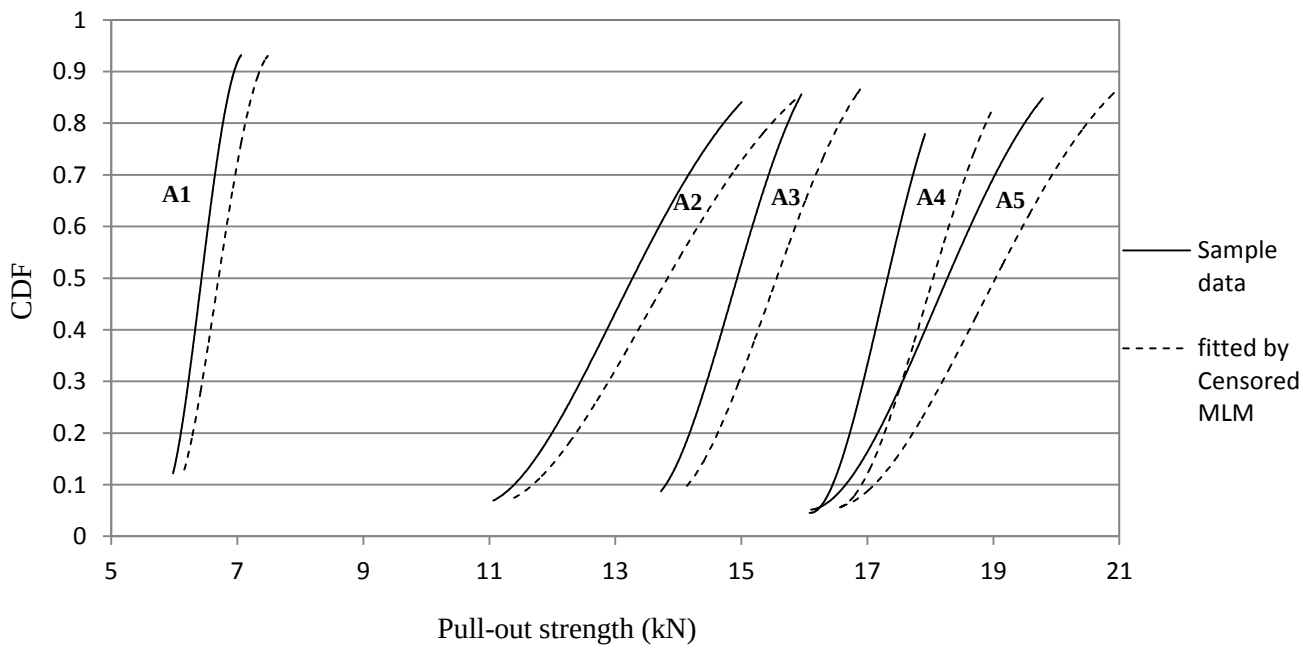

Figure A. 6- CDF with parameters estimated using sample data and censored MLM for specimens of type A

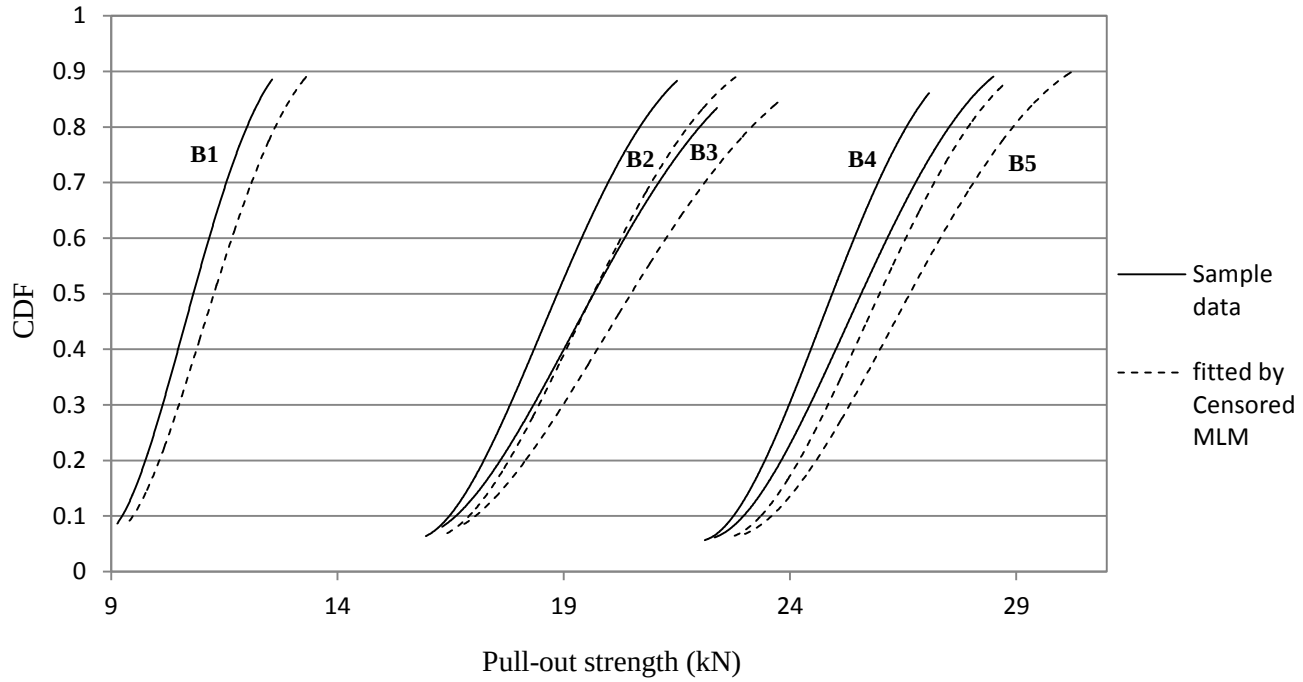

Figure A. 7- CDF with parameters estimated using sample data and censored MLM for specimens of type B

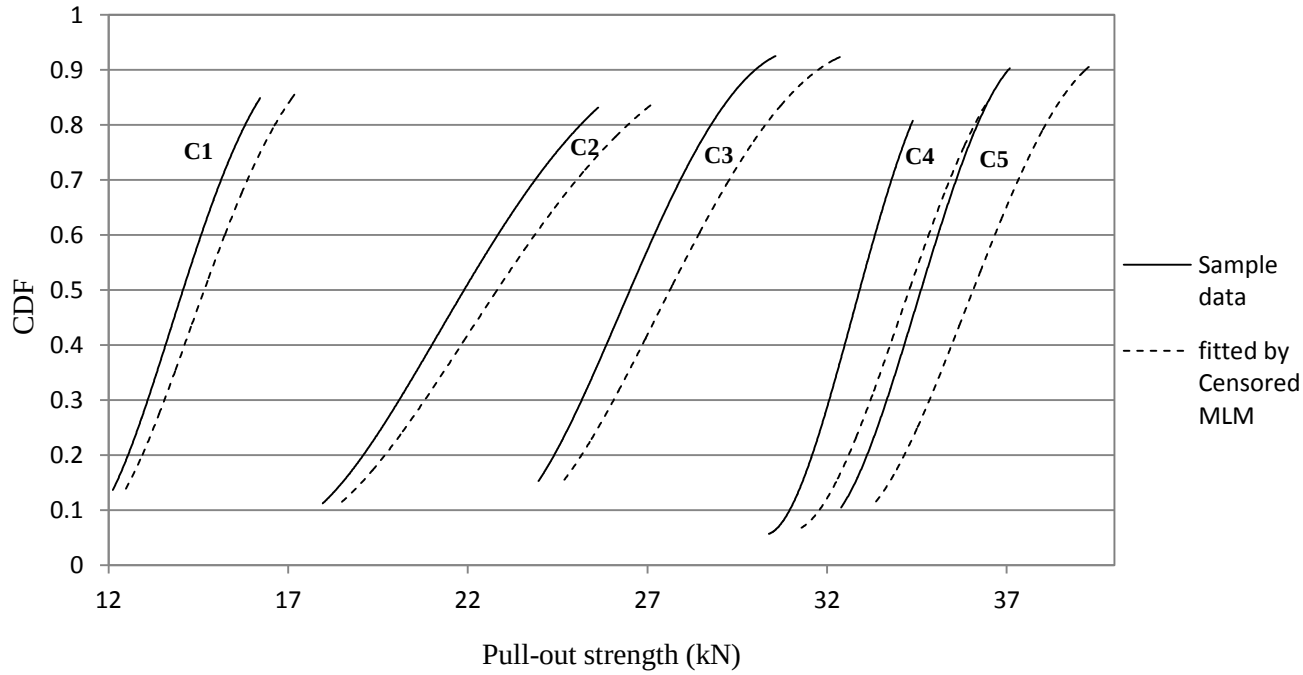

Figure A. 8- CDF with parameters estimated using sample data and censored MLM for specimens of type C

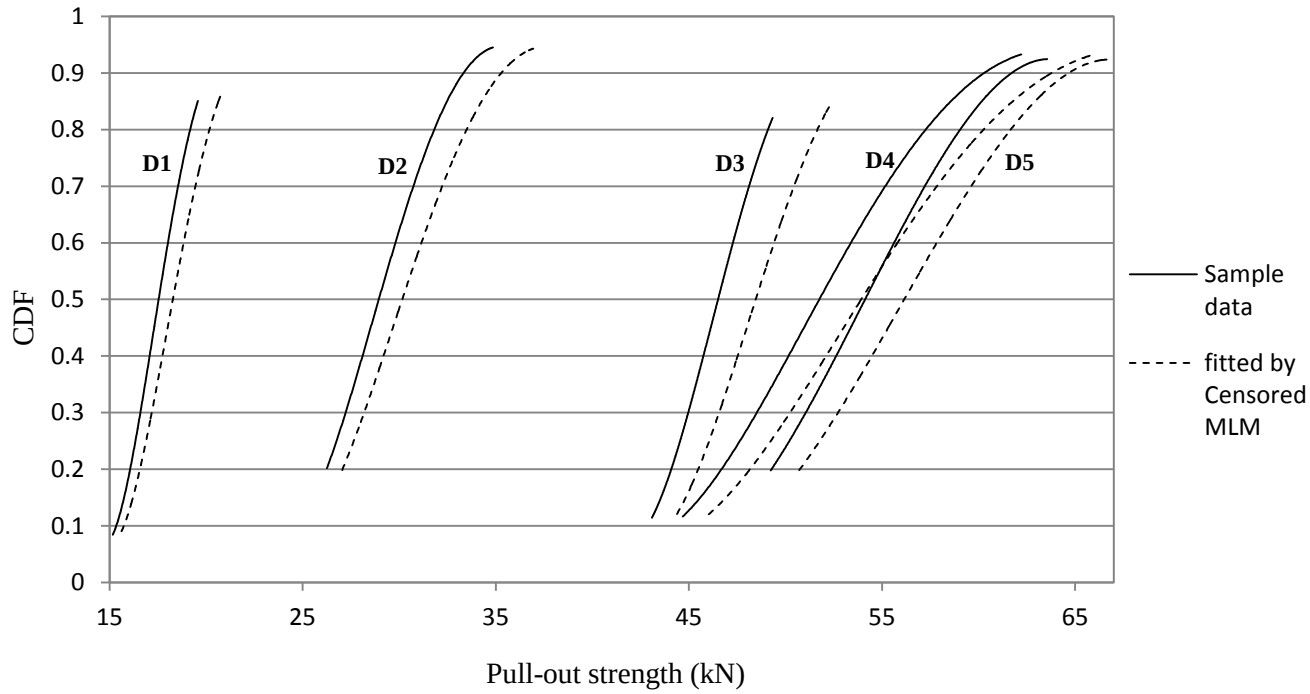

Figure A. 9- CDF with parameters estimated using sample data and censored MLM for specimens of type D

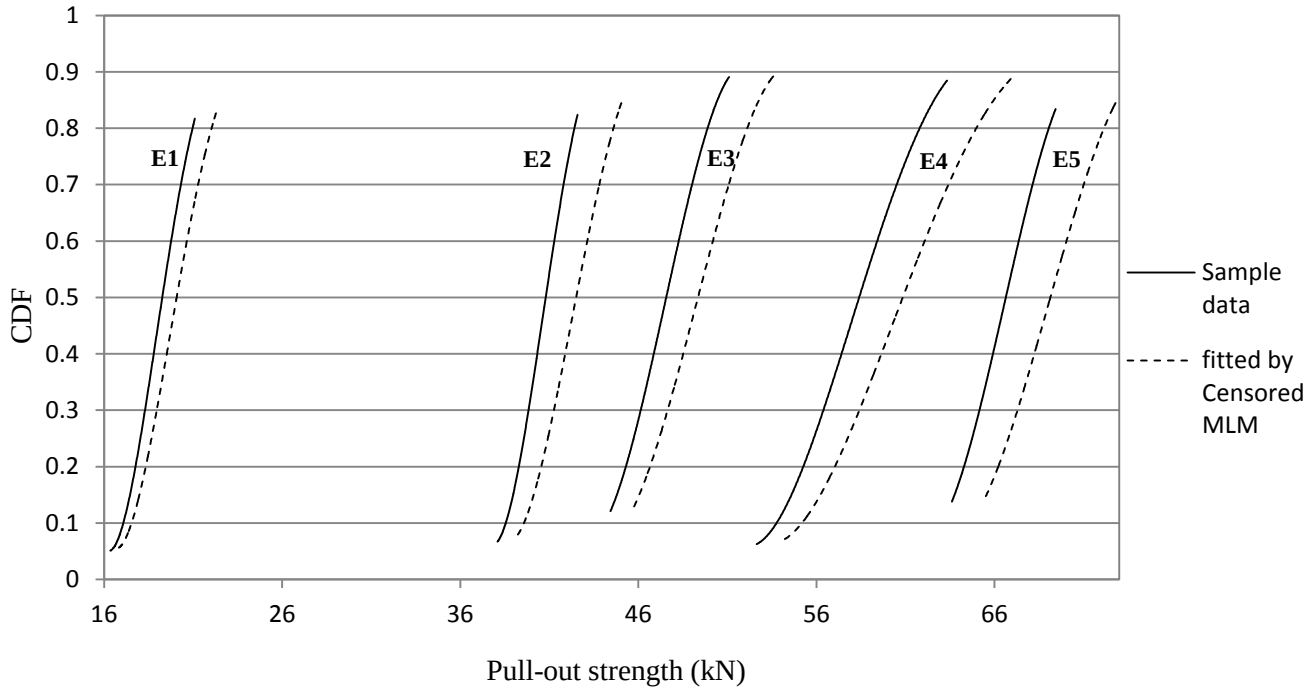

Figure A. 10- CDF with parameters estimated using sample data and censored MLM for specimens of type E

Appendix B. PHOTOGRAPHS

Figure B. 1- Specimens are drilled and prepared for gluing procedure

Figure B. 2- Rods are prepared for gluing procedure

Figure B. 3- A suitable foam tape was used at the end of the rods in order to center the rod in the hole

Figure B. 4- Specimens and rods are ready for gluing procedure

Figure B. 5- The adhesive was injected into the base of the holes by using the injection gun

Figure B. 6- The rods were glued into the predrilled holes by continuous pressure and rotating

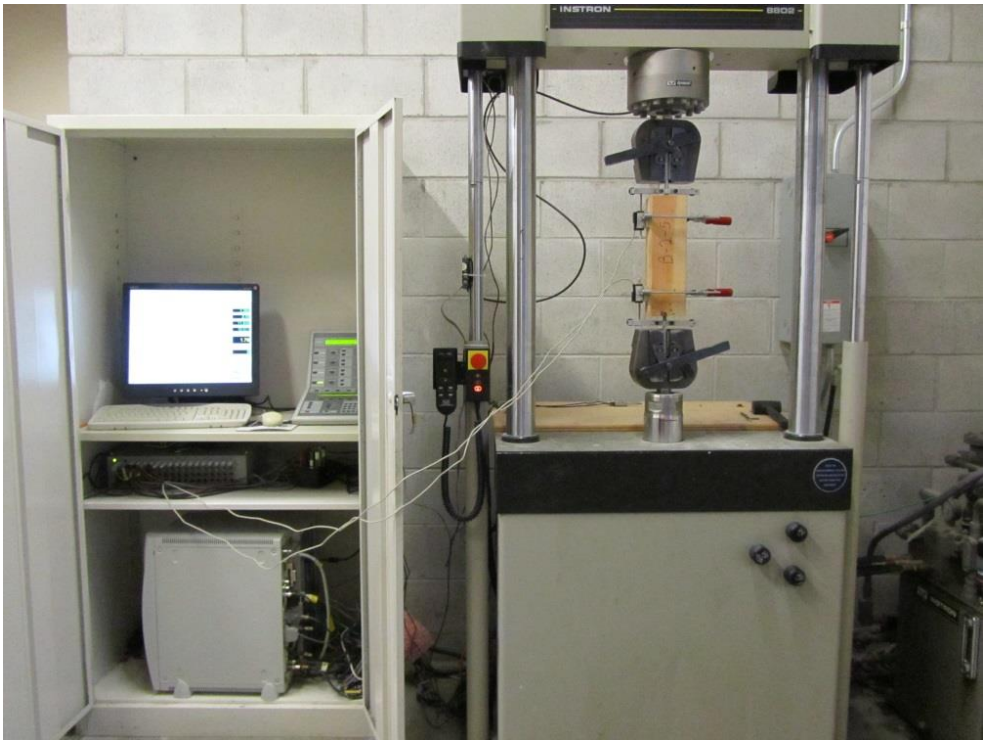

Figure B. 7- Machine and testing device of the samples

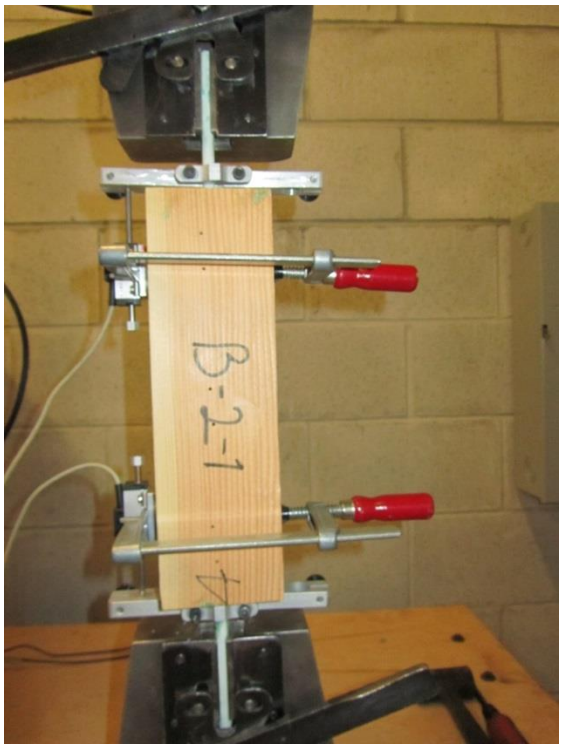

Figure B. 8- Testing of the specimens. Two LVDTs were installed at both ends

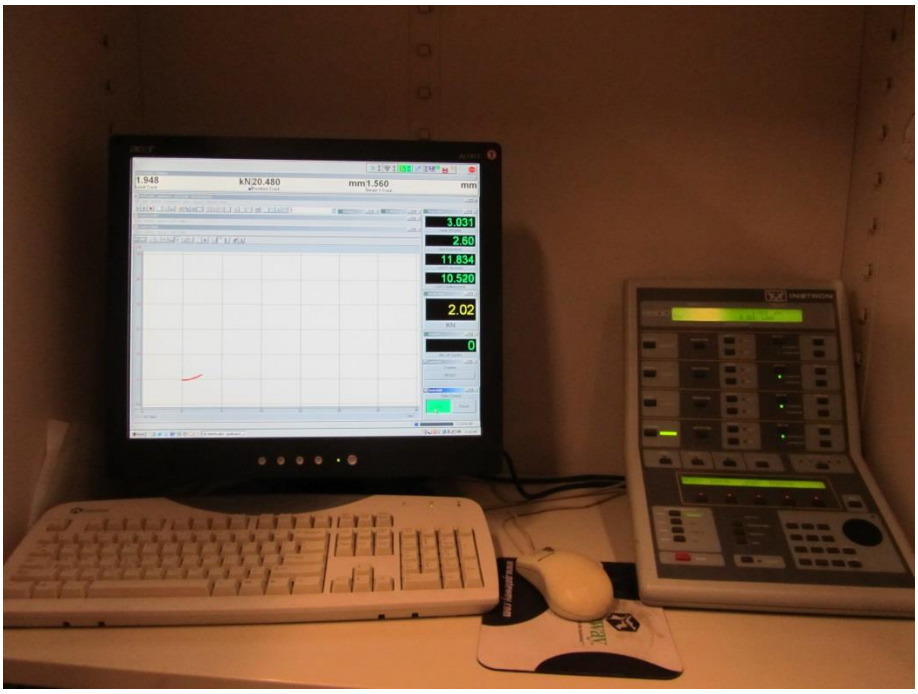

Figure B. 9- Computer and electronic devices for recording load and displacement data

Appendix C. NUMERICAL MODELING RESULTS

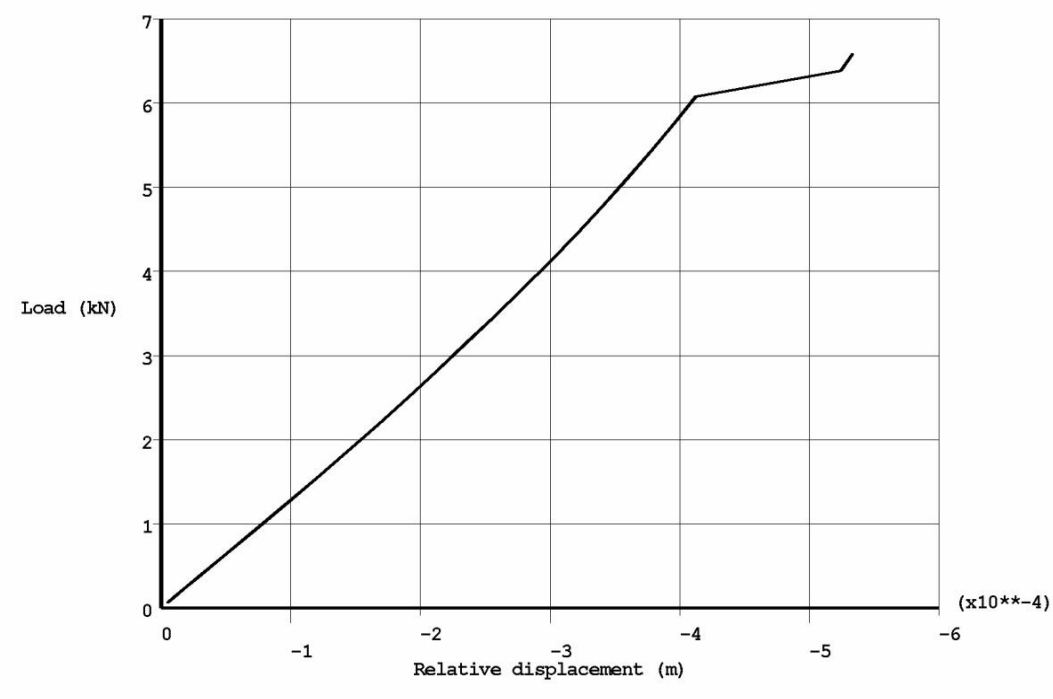

Figure C. 1- Load-displacement curve from FEA for specimen of type A1

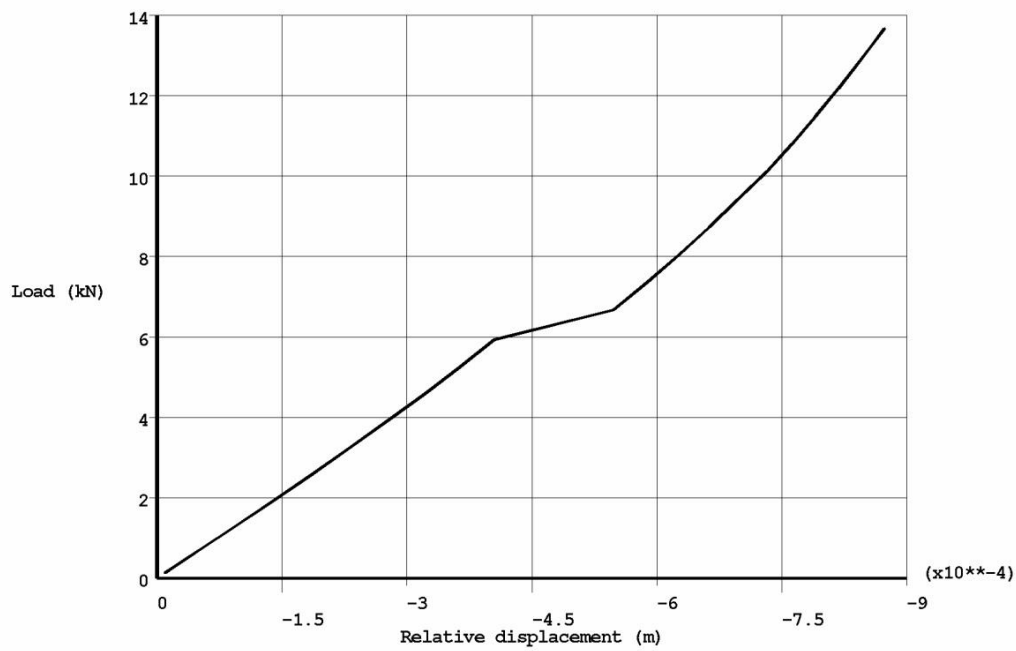

Figure C. 2- Load-displacement curve from FEA for specimen of type A2

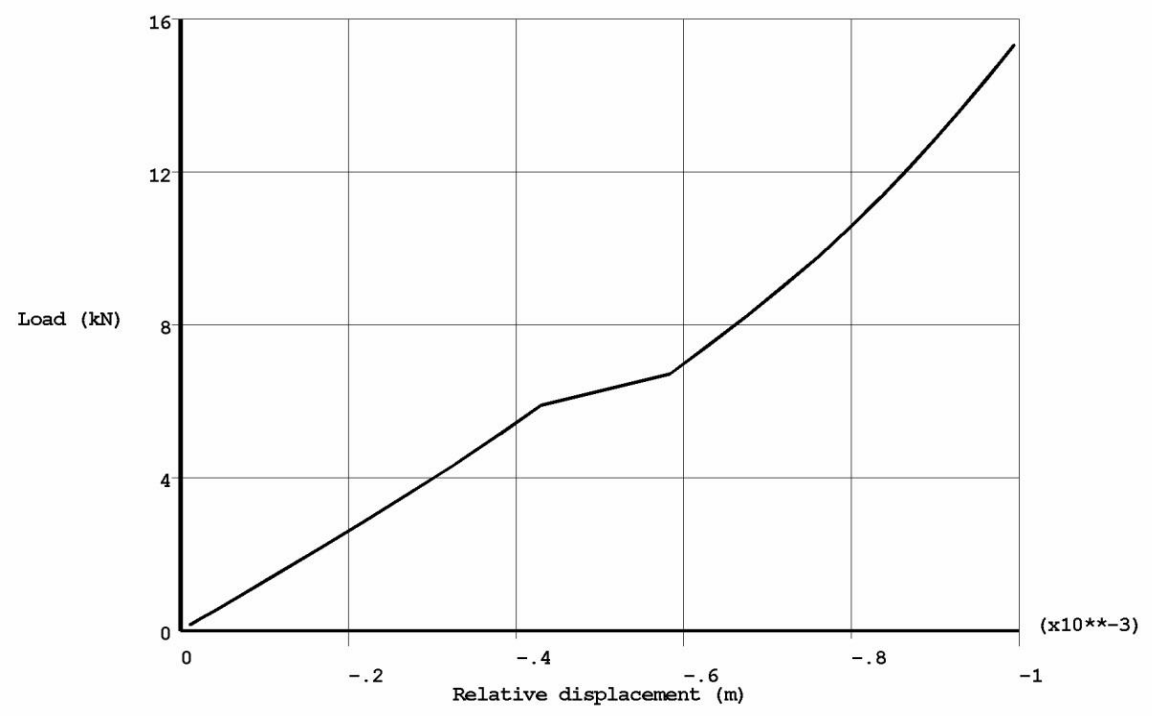

Figure C. 3- Load-displacement curve from FEA for specimen of type A3

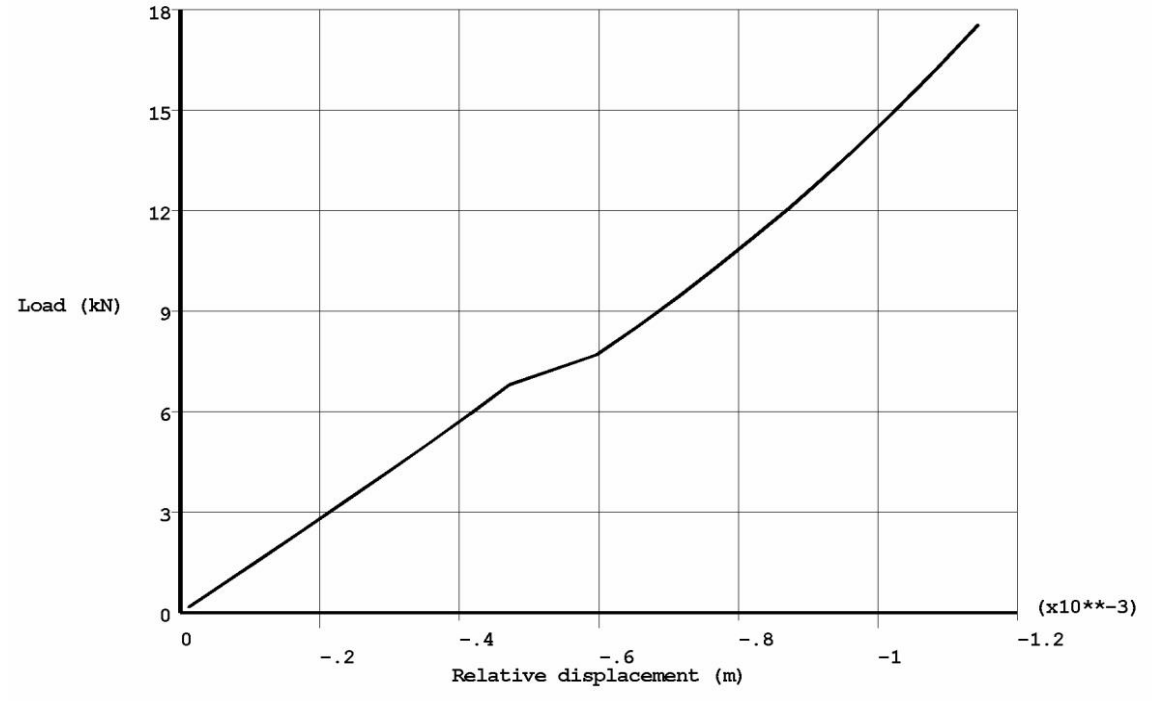

Figure C. 4- Load-displacement curve from FEA for specimen of type A4

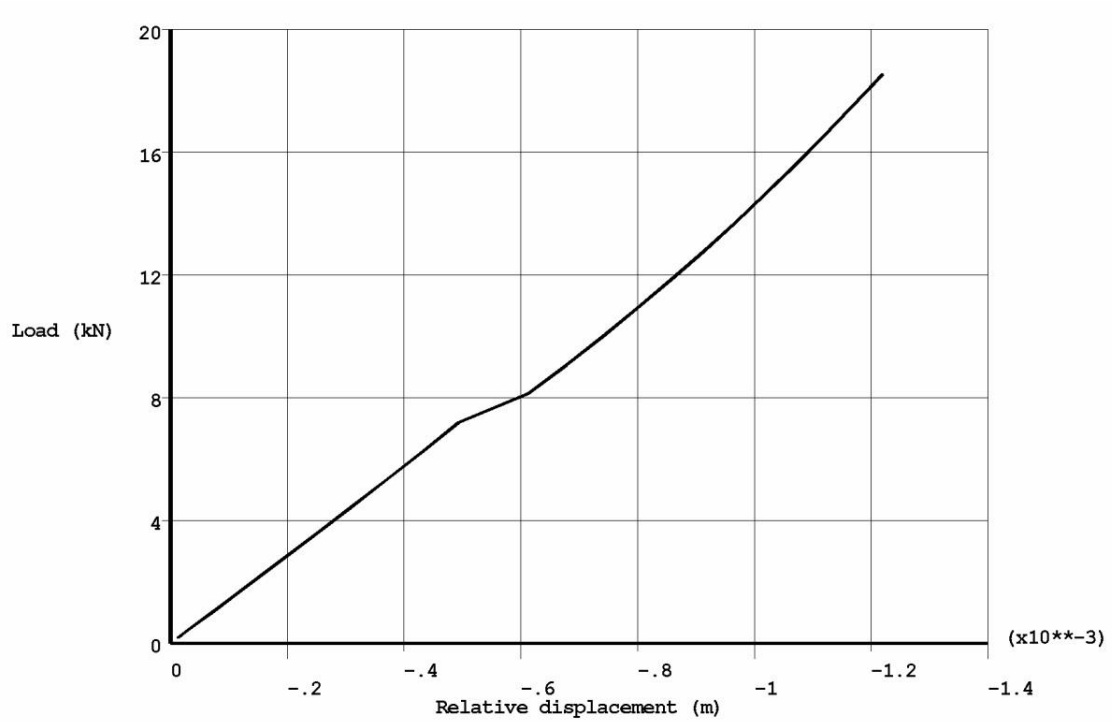

Figure C. 5- Load-displacement curve from FEA for specimen of type A5

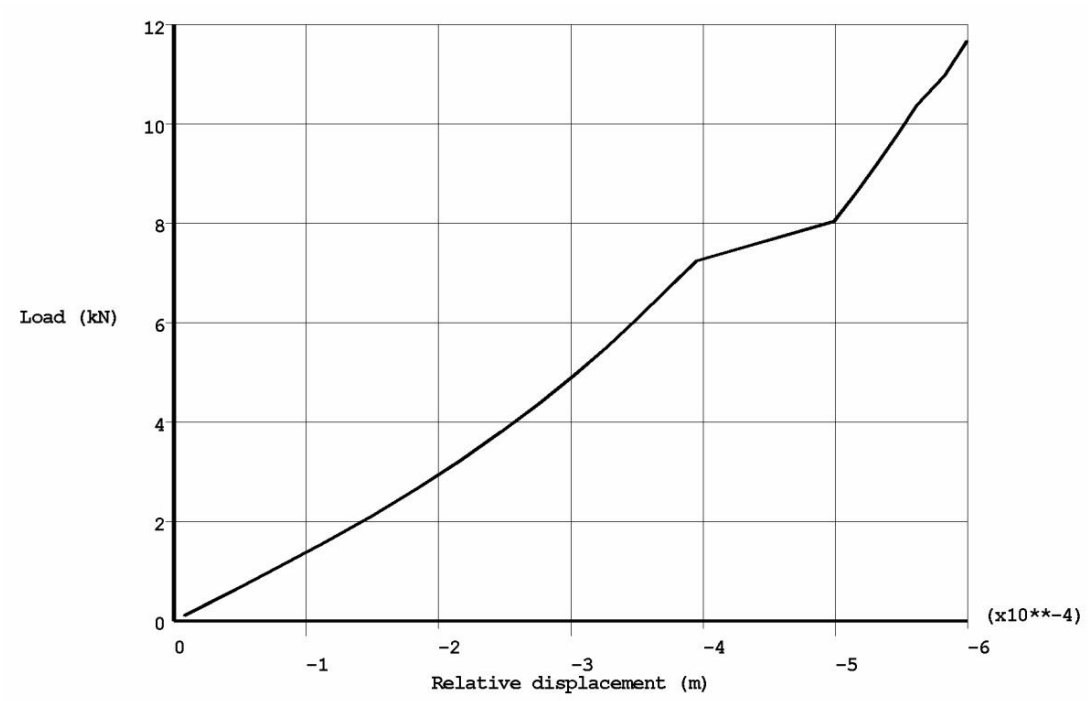

Figure C. 6- Load-displacement curve from FEA for specimen of type B1

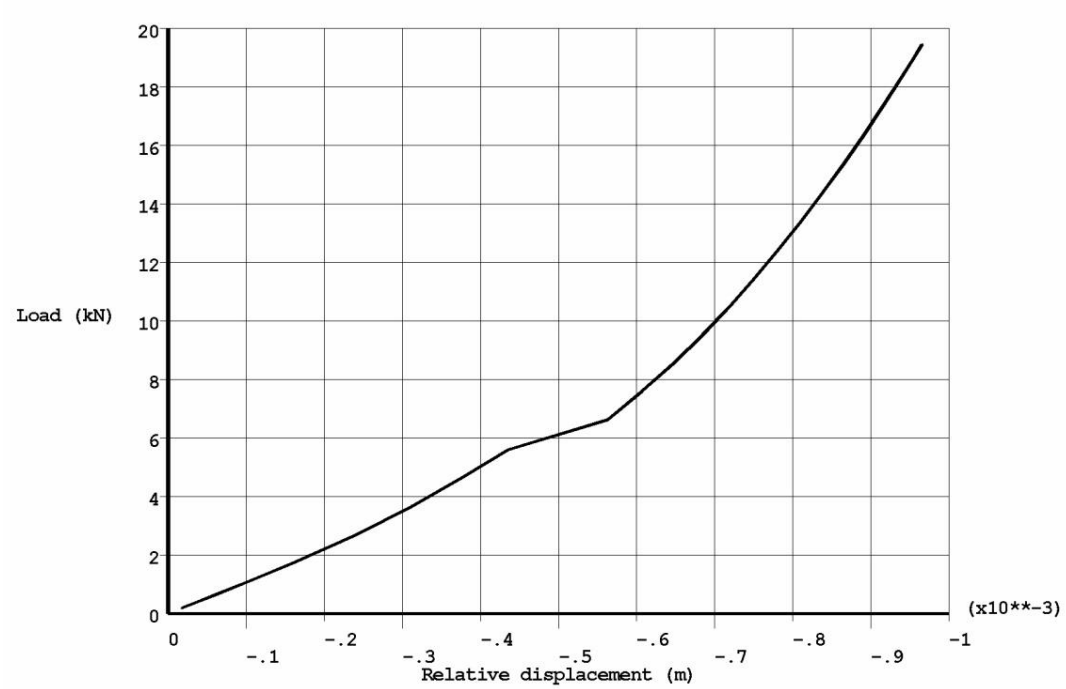

Figure C. 7- Load-displacement curve from FEA for specimen of type B2

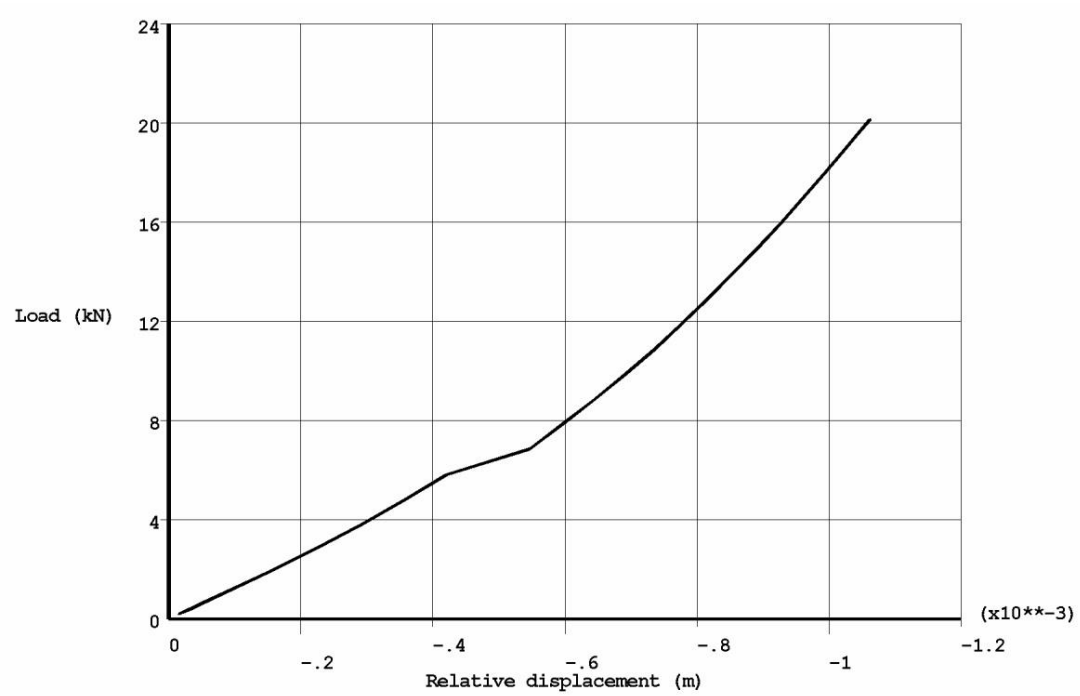

Figure C. 8- Load-displacement curve from FEA for specimen of type B3

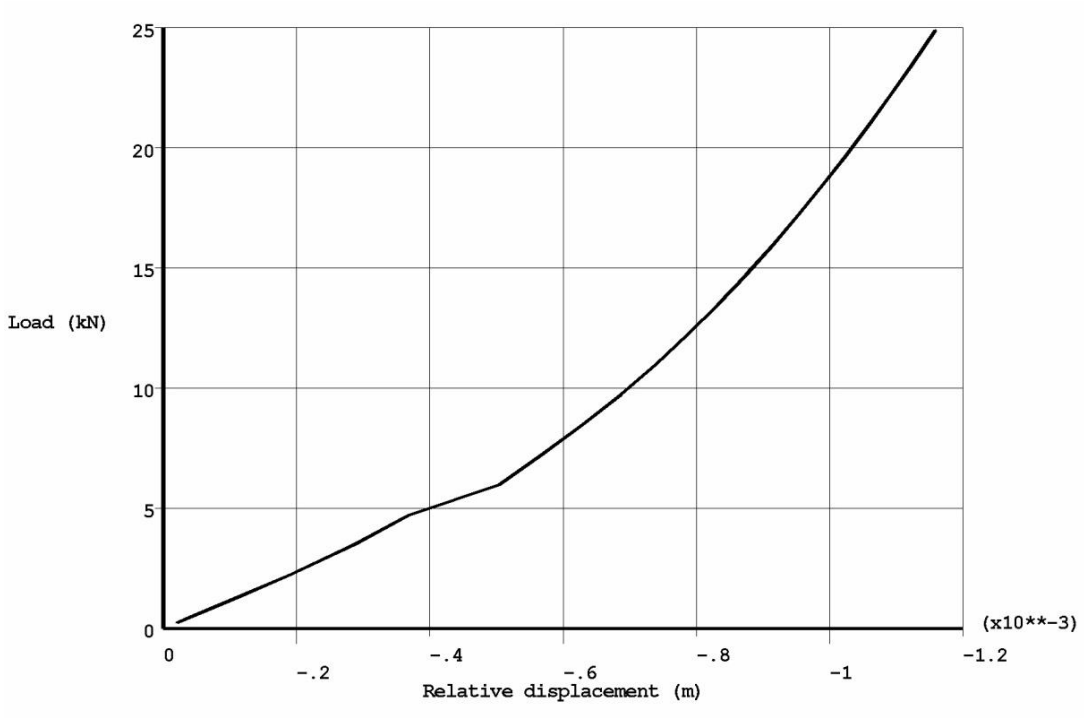

Figure C. 9- Load-displacement curve from FEA for specimen of type B4

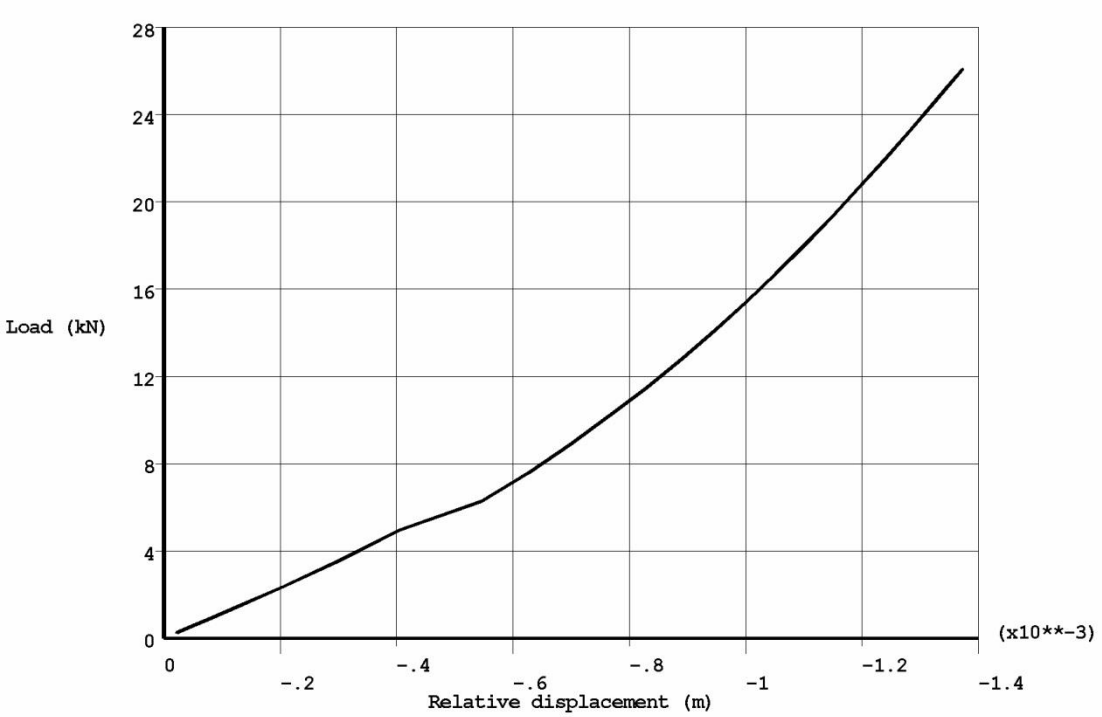

Figure C. 10- Load-displacement curve from FEA for specimen of type B5

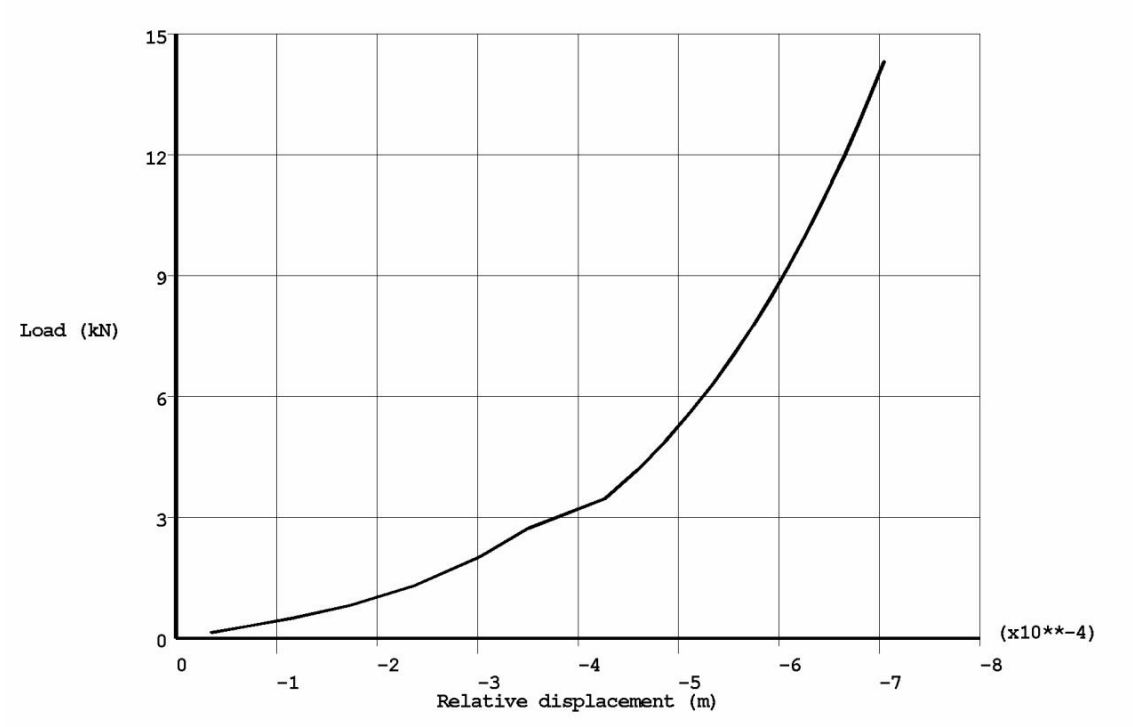

Figure C. 11- Load-displacement curve from FEA for specimen of type C1

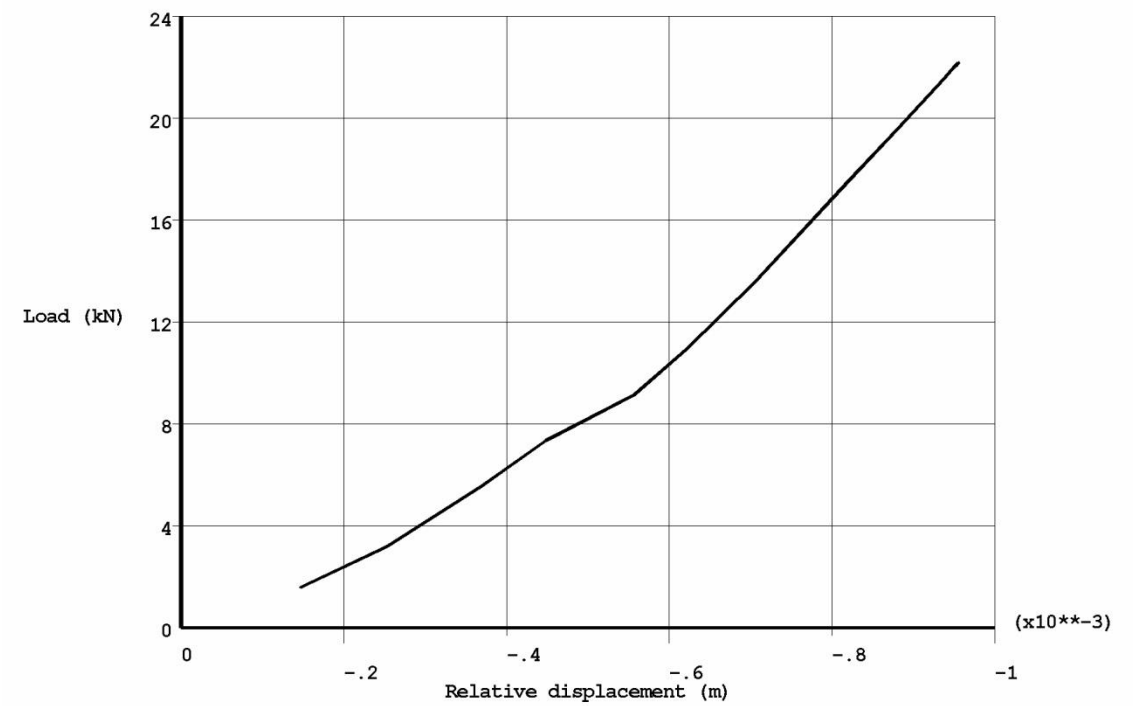

Figure C. 12- Load-displacement curve from FEA for specimen of type C2

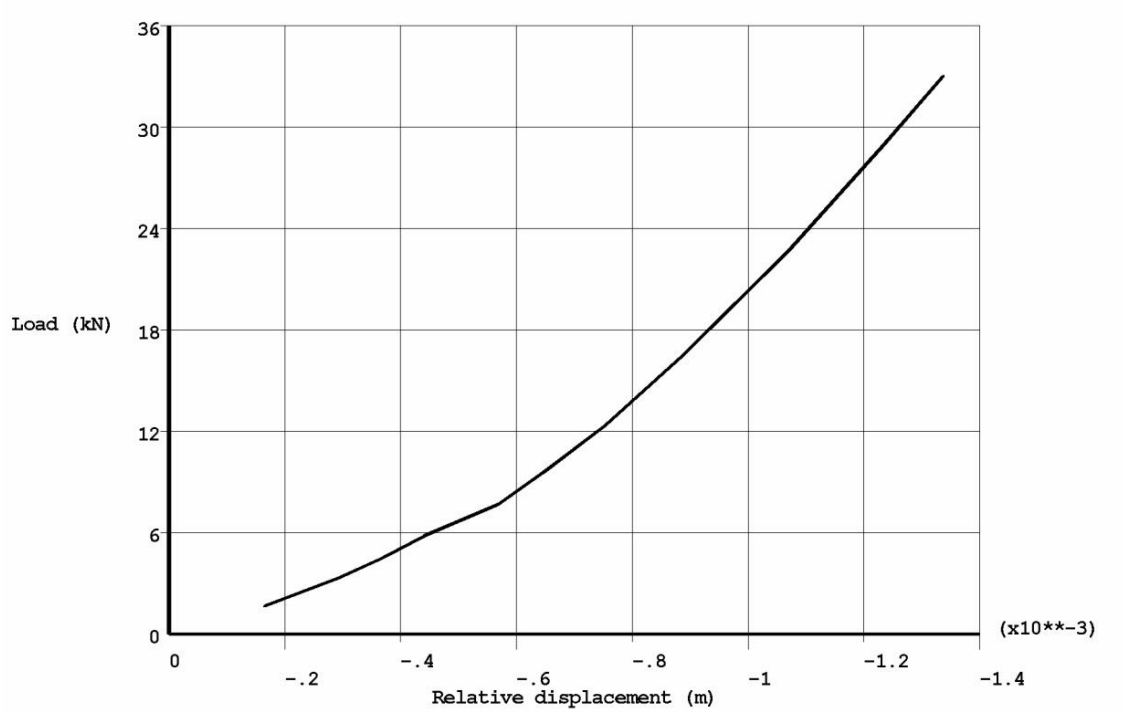

Figure C. 13- Load-displacement curve from FEA for specimen of type C4

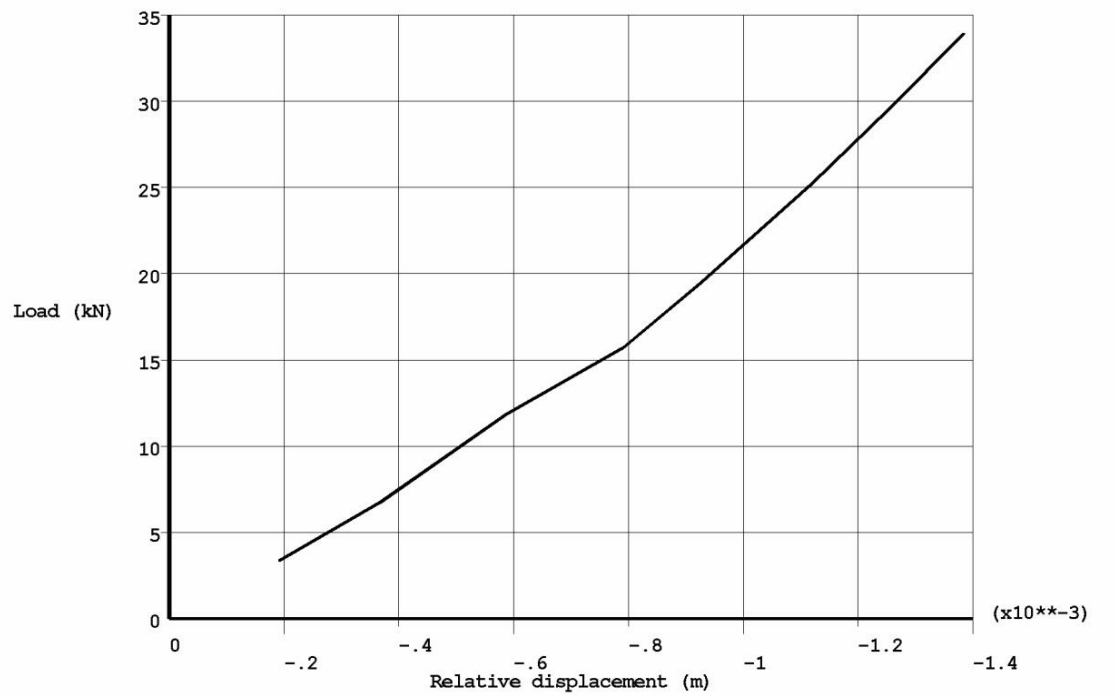

Figure C. 14- Load-displacement curve from FEA for specimen of type C5

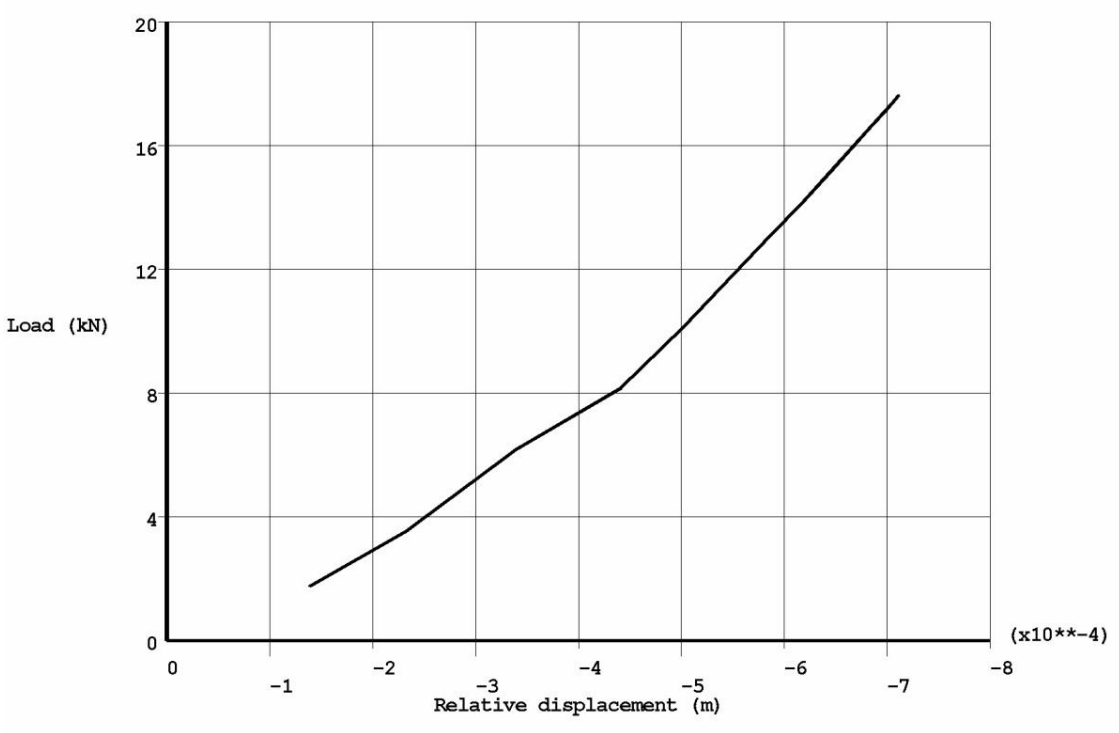

Figure C. 15- Load-displacement curve from FEA for specimen of type D1

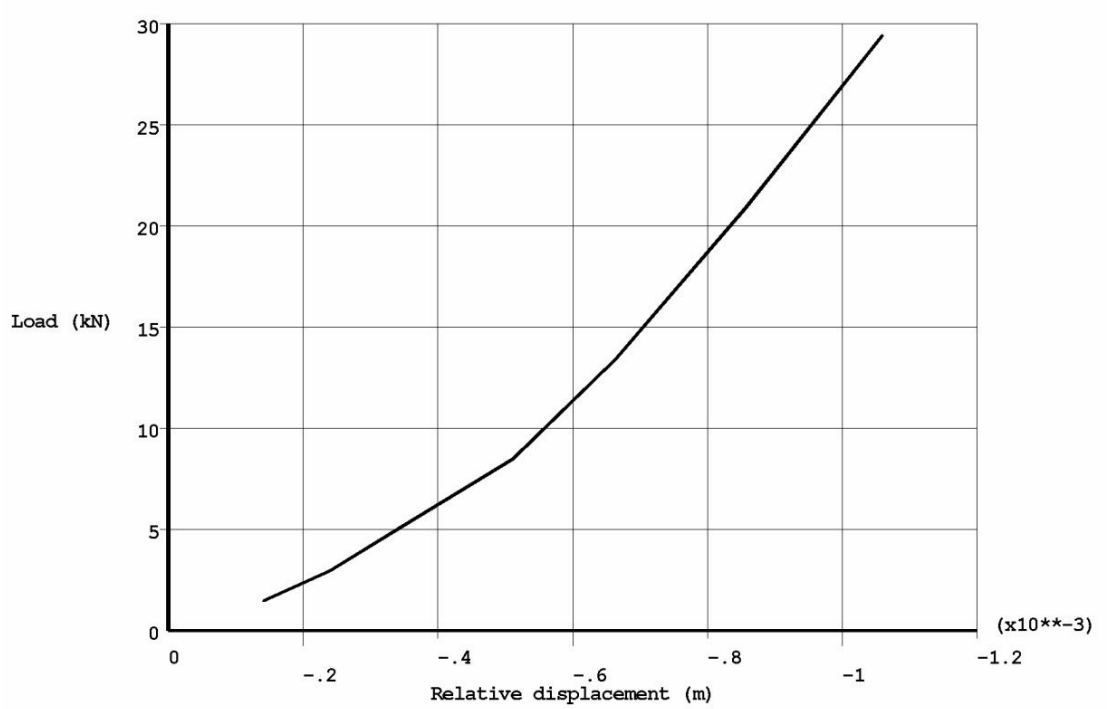

Figure C. 16- Load-displacement curve from FEA for specimen of type D2

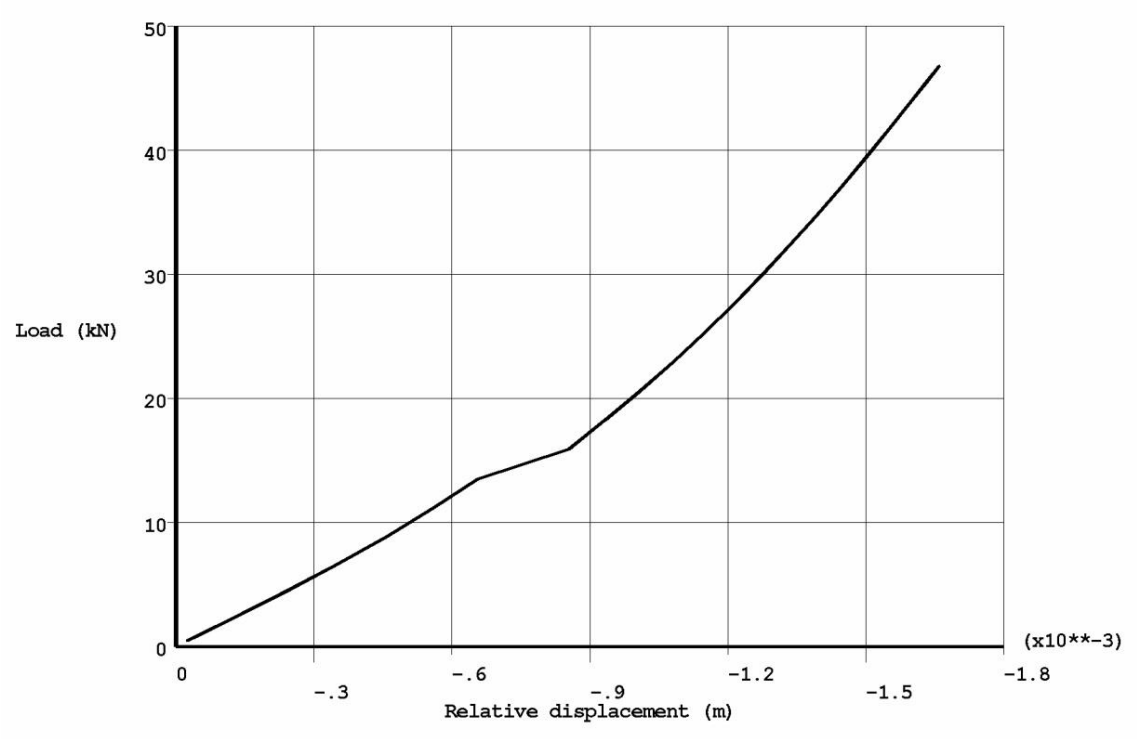

Figure C. 17- Load-displacement curve from FEA for specimen of type D3

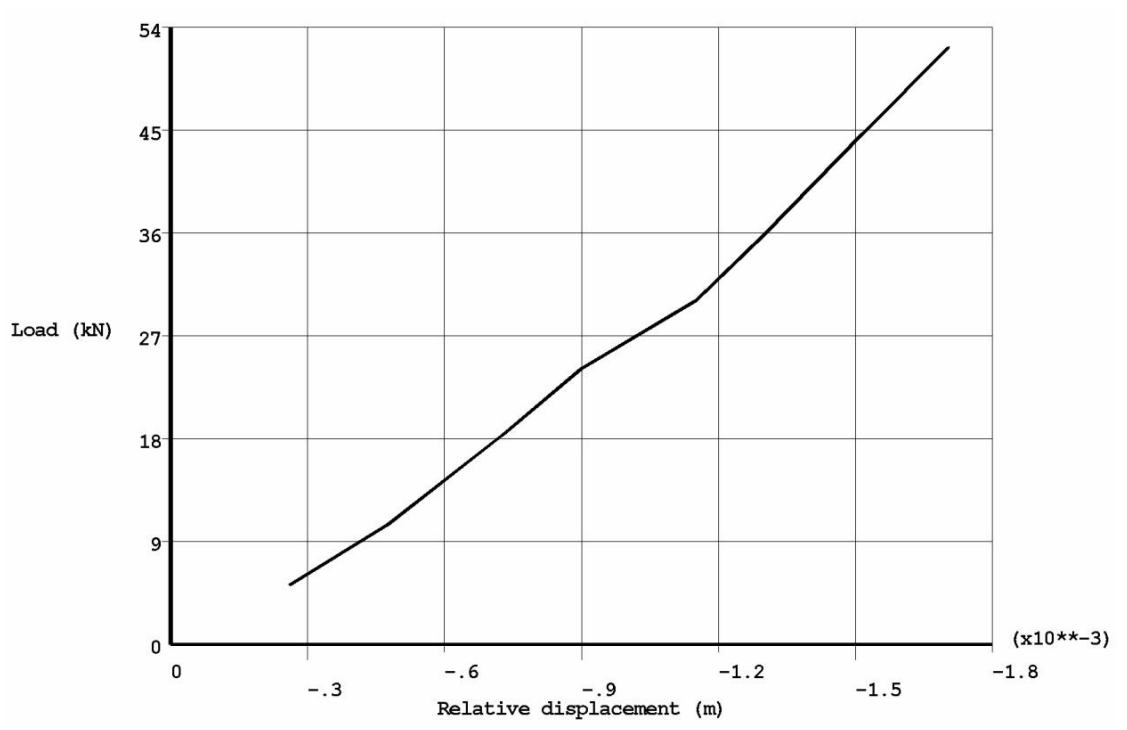

Figure C. 18- Load-displacement curve from FEA for specimen of type D4

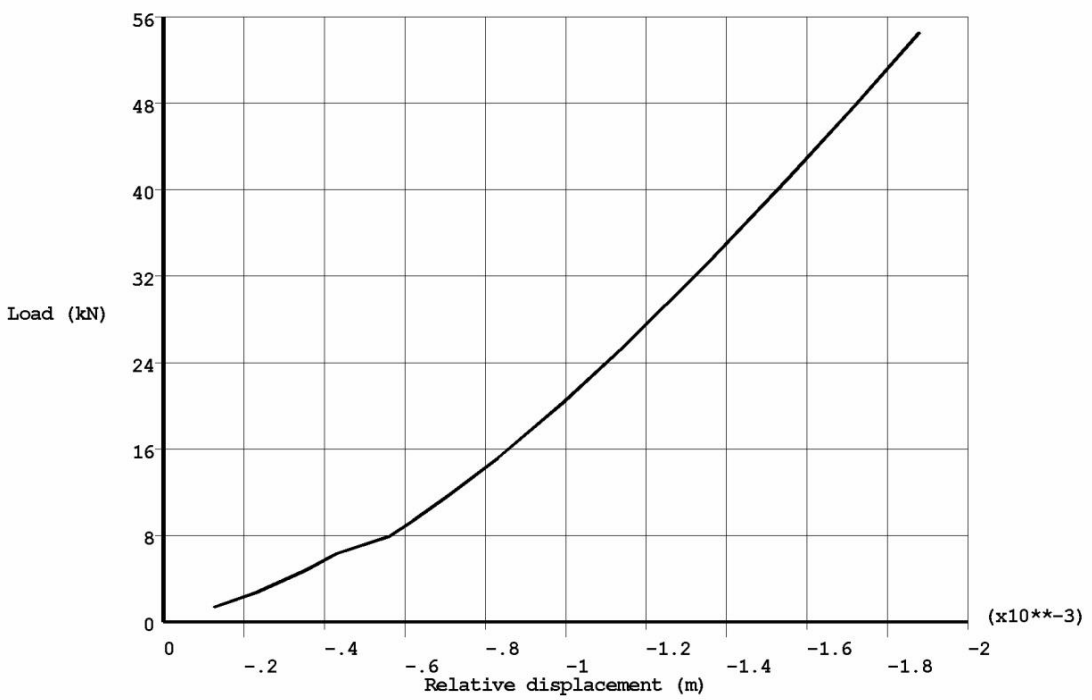

Figure C. 19- Load-displacement curve from FEA for specimen of type D5

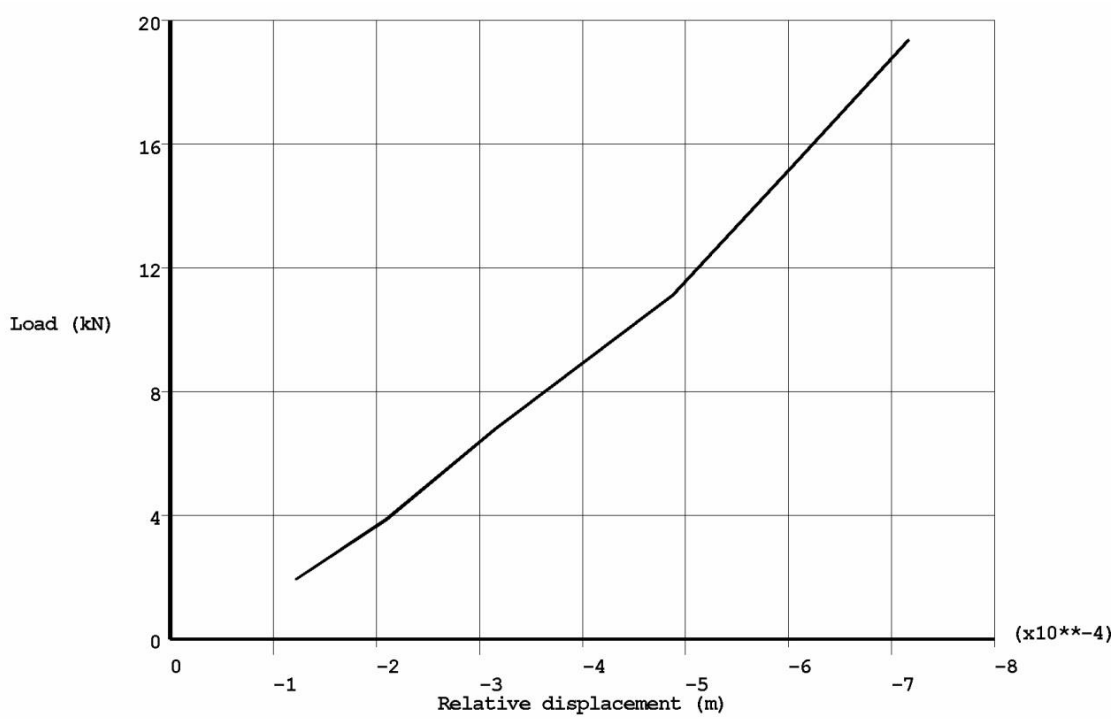

Figure C. 20- Load-displacement curve from FEA for specimen of type E1

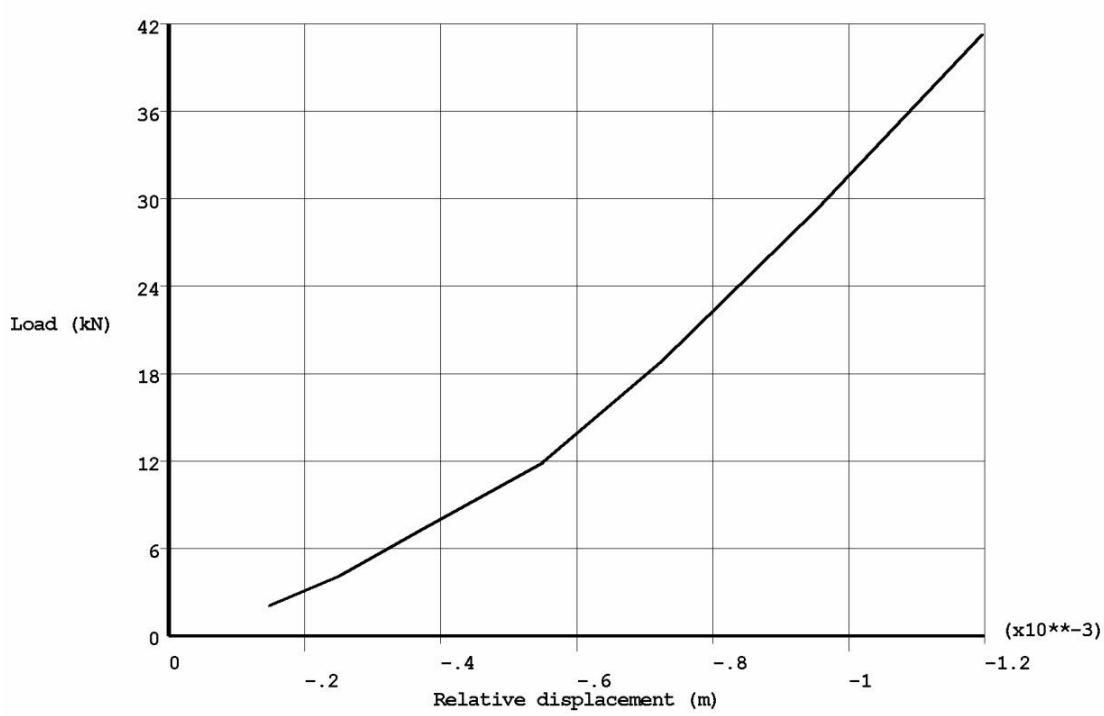

Figure C. 21- Load-displacement curve from FEA for specimen of type E2

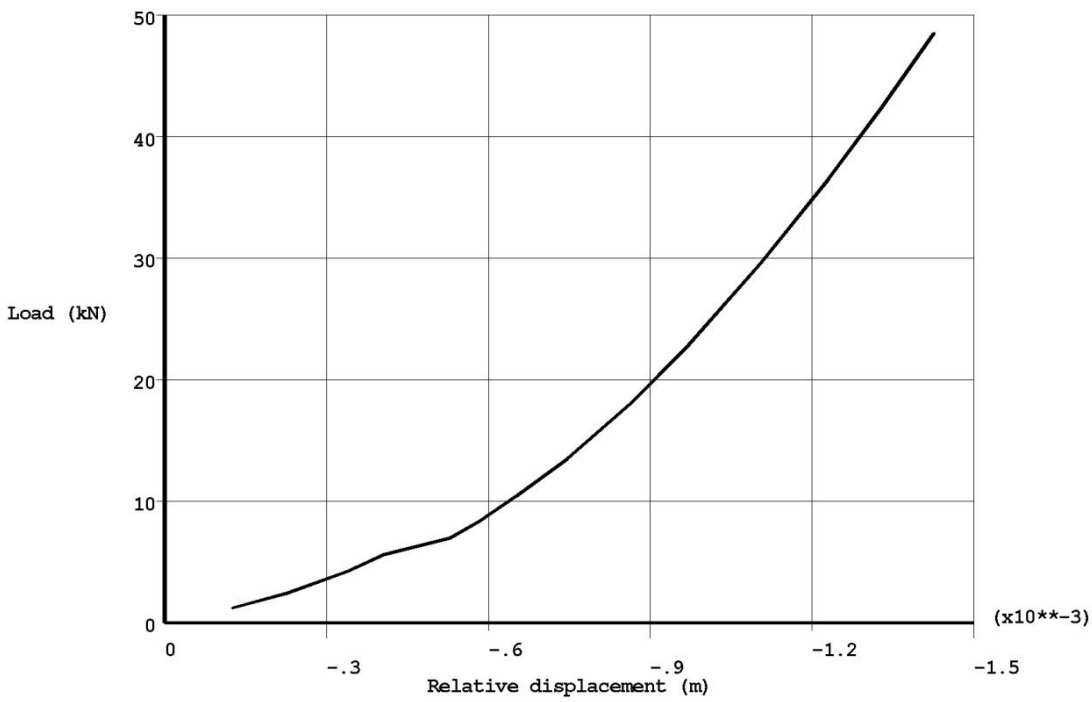

Figure C. 22- Load-displacement curve from FEA for specimen of type E3

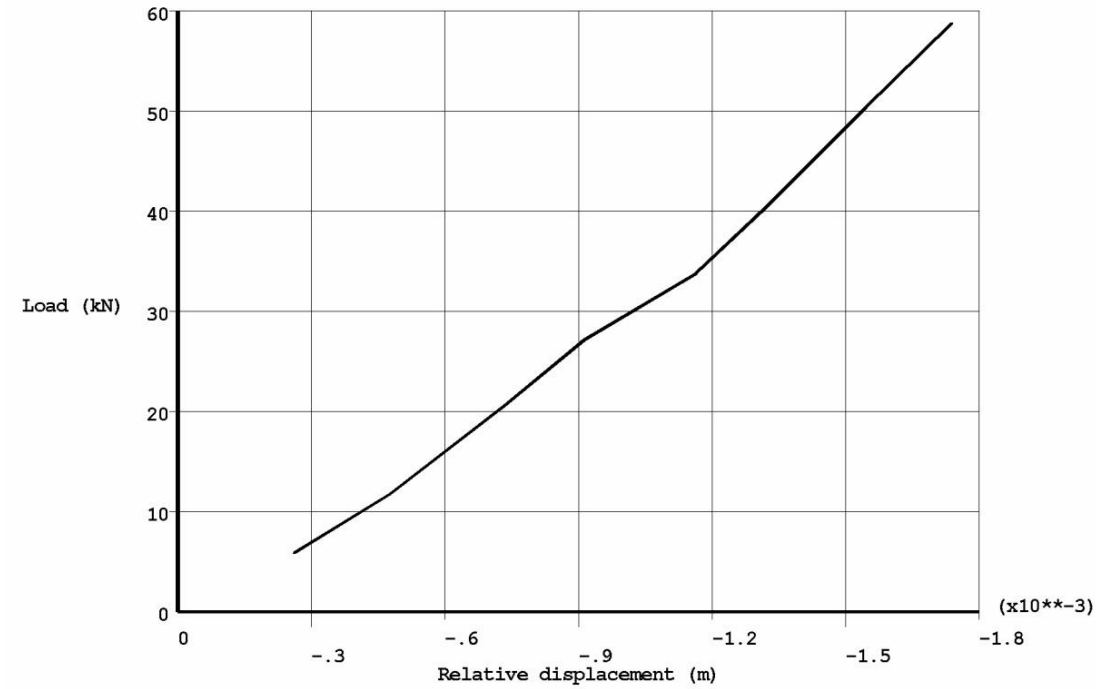

Figure C. 23- Load-displacement curve from FEA for specimen of type E4

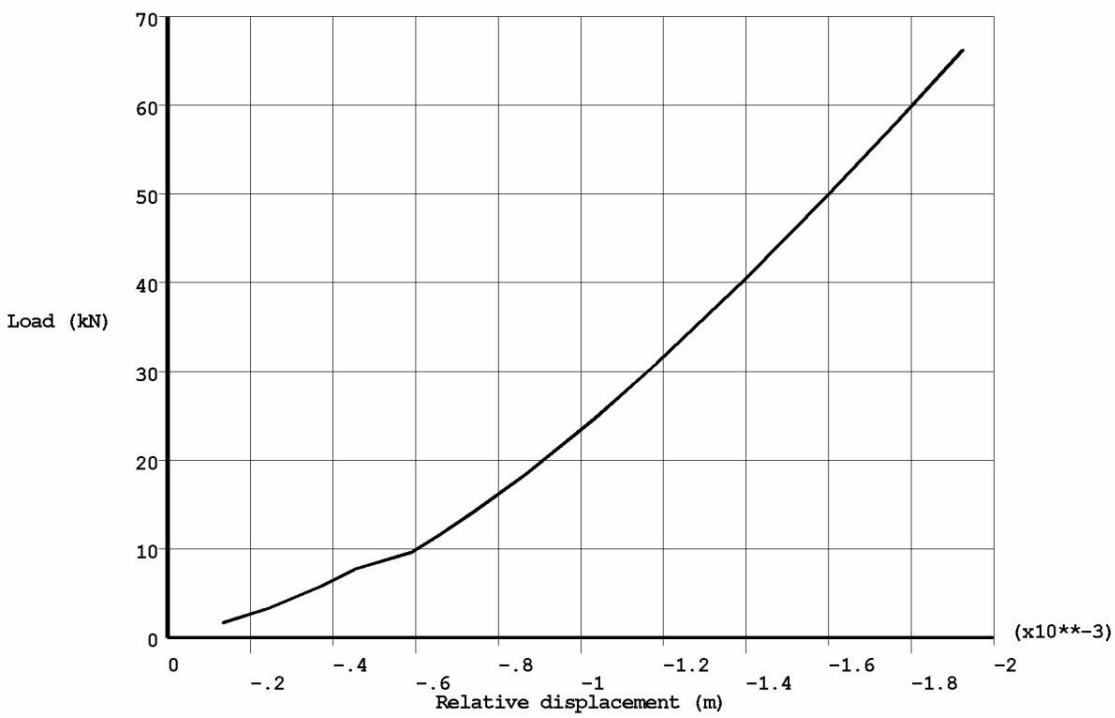

Figure C. 24- Load-displacement curve from FEA for specimen of type E5

Ineffective numerical modeling trials

In the process of reaching to a reliable numerical model with ANSYS, some trials have been done which were ineffective and unable to predict the structural performance of timber joints with glued-in rods.

One approach was to model the bond-line with glue command, which made the rod and timber specimen as an integrated volume. This means that the adhesive material does not act in sliding mode like they actually do in the experiment.

Another model has been tested using the surface to surface contact technology, which applied directly between rod and the timber without defining any gap for adhesive. The stress distribution results was acceptable, however the deformations was too larger than that of the experiments. Since there was no physically adhesive material in the model, it was also not an effective model in predicting adhesive behavior.

Finally the layer of adhesive was defined between the timber and the rod; then the surface to surface contact technology was applied to the rod-adhesive and adhesive-timber interface. Several trial models with different parameters of contact bond were tested. At the beginning, FKP constant was set to 1×10^{10} and μ to 0.3, but there was no convergence in the solution. Then these parameters were increased stepwise until the final model has been attained with good convergence and prediction accuracy.